



ARC Centre of Excellence in Population Ageing Research

Working Paper 2017/02

Pricing and Hedging Guaranteed Minimum Withdrawal Benefits under a General Lévy Framework using the COS Method

Jennifer Alonso-García¹, Oliver Wood² and Jonathan Ziveyi³.

¹Research Fellow, ARC Centre of Excellence in Population Ageing Research (CEPAR), UNSW Business School, UNSW Sydney, email: j.alonsogarcia@unsw.edu.au

²CommInsure, 48 Martin Pl, Sydney NSW 2000, Australia. email: oliver.wood95@gmail.com

³Senior Lecturer and CEPAR Associate Investigator, School of Risk and Actuarial Studies, UNSW Business School, UNSW Sydney, email: j.ziveyi@unsw.edu.au

This paper can be downloaded without charge from the ARC Centre of Excellence in Population Ageing Research Working Paper Series available at www.cepar.edu.au

Pricing and hedging guaranteed minimum withdrawal benefits under a general Lévy framework using the COS method

Jennifer Alonso-García*
Oliver Wood†
Jonathan Ziveyi‡

February 10, 2017

Abstract

This paper extends the Fourier-cosine (COS) method to the pricing and hedging of variable annuities embedded with guaranteed minimum withdrawal benefit (GMWB) riders. The COS method facilitates efficient computation of prices and hedge ratios of the GMWB riders when the underlying fund dynamics evolve under the influence of the general class of Lévy processes. Formulae are derived to value the contract at each withdrawal date using a backward recursive dynamic programming algorithm. Numerical comparisons are performed with results presented in Bacinello et al. (2014) and Luo and Shevchenko (2014) to confirm the accuracy of the method. The efficiency of the proposed method is assessed by making comparisons with the approach presented in Bacinello et al. (2014). We find that the COS method presents highly accurate results with notably fast computational times. The valuation framework forms the basis for GMWB hedging. A local risk minimisation approach to hedging inter-withdrawal date risks is developed. A variety of risk measures are considered for minimisation in the general Lévy framework. While the second moment and variance have been considered in existing literature, we show that the value-at-risk may also be of interest as a risk measure to minimise risk in variable annuities portfolios.

Keywords: Variable annuity, GMWB, COS method, hedging, risk minimisation

1 Introduction

The global market for variable annuities (VAs) represents a huge pool of assets. For instance, the market share of VAs in the U.S. as of the second quarter of 2015 was estimated to be US\$1.98 trillion (IRI, 2015). These VAs are a popular retirement product for several reasons, including equity exposure, longevity protection, and the various guaranteed minimum benefits (GMBs)

This project has received funding from the ARC Center of Excellence in Population Ageing Research (grant CE110001029). We thank attendees at the Quantitative Methods in Finance conference 2016 and the University of New South Wales for useful comments. The authors are responsible for any errors.

* (Corresponding author). ARC Centre of Excellence in Population Ageing Research (CEPAR), University of New South Wales, Level 3, East Wing, 223 Anzac Parade, Kensington NSW 2033, Australia. Email: j.alonsogarcia@unsw.edu.au

† CommInsure, 48 Martin Pl, Sydney NSW 2000, Australia. Email: oliver.wood95@gmail.com

‡ School of Risk and Actuarial Studies, Business School, University of New South Wales, Sydney, NSW 2052, Australia and ARC Centre of Excellence in Population Ageing Research (CEPAR), University of New South Wales, Level 3, East Wing, 223 Anzac Parade, Kensington NSW 2033, Australia. Email: j.ziveyi@unsw.edu.au

that insurers offer to protect their customers from downside market risks (Hanif et al., 2007; Condron, 2008).

Guaranteed minimum withdrawal benefits (GMWBs) are the most popular form of GMBs, which come in various forms including the guaranteed lifelong withdrawal benefit (GLWB), an alternative that guarantees a fixed periodic withdrawal amount until death of the policyholder (Bauer et al., 2008; Ledlie et al., 2008; Fung et al., 2014). These ensure a minimum withdrawal amount at each withdrawal date over the term of the contract, regardless of the status of the VA investment account. The insurer funds this guarantee with proportional, periodic charges to the investment account.

The valuation of GMWBs is first considered in the academic literature by Milevsky and Salisbury (2006). The authors recognise the sensitivity of the value of GMWBs to policyholder behaviour. In practice, GMWB policyholders are able to choose how much to withdraw from their accounts or whether to surrender the contract, corresponding to the full withdrawal of the VA account. Milevsky and Salisbury (2006) define two types of policyholder withdrawal behaviours – *static* and *dynamic*. Static policyholders withdraw at the constant guaranteed withdrawal rate, whereas dynamic policyholders are entirely rational and maximise the value of the GMWB by potentially surrendering the contract early or making partial withdrawals.

Due to the complicated nature of the option-like features of GMWBs, Milevsky and Salisbury (2006) make several simplifying assumptions to value the contract in the static case. A notable simplification is modelling the fund dynamics with geometric Brownian motion (GBM), which is known to underestimate the tails of asset return distribution and assumes constant volatility and interest rates (Kélani and Quittard-Pinon, 2015). Other simplifications include continuous withdrawals and ignoring mortality risk.

The authors show that the contract can be bifurcated into a quanto Asian put and a term-annuity certain which can be valued using standard numerical techniques. Under the same simplifying assumptions, Dai et al. (2008) and Chen and Forsyth (2008) set up a singular and an impulse stochastic optimal control problem. These techniques lead to solving Hamilton-Jacobi-Bellman (HJB) equations using finite differencing techniques.

Using the numerical scheme presented in Chen and Forsyth (2008), Chen et al. (2008) provide further analysis on the effect of various parameters on the price of GMWB riders. This analysis includes studying the effects of the volatility parameter, a separate mutual fund fee, sub-optimal policyholder behaviour, time to maturity, time between withdrawals, varying interest rates and the use of a jump-diffusion process on the GMWB’s fair fee. Their results strengthen the findings of Milevsky and Salisbury (2006), by showing that only under several simultaneous unrealistic assumptions would the industry insurance fees at the time be enough to cover the expense of the GMWB contract.

Various pricing techniques adapted from the quantitative finance literature have also been applied to the problem of pricing GMWBs. For example, Peng et al. (2012) assume GBM asset dynamics but allow for stochastic interest rates evolving according to the Vasicek (1977) model and then use a combination the Roger-Shi’s technique and Thompson’s method to find lower and upper bounds for the fair fee, respectively (Rogers and Shi, 1995; Thompson, 1999). Another example is a “tree” based method presented in Yang and Dai (2013), where the authors again assume GBM. Both papers show that the fair fee is highly dependent on the volatility of the stochastic interest rate and instantaneous correlation between the underlying and the interest rate. They argue that the stochastic interest rate assumption is especially important for long-dated contracts.

Bacinello et al. (2014) consider the valuation of the GMWB rider when the underlying fund dynamics evolve under the influence of Lévy processes. The valuation problem is formulated as

a dynamic programming algorithm, which is solved by using the Fast Fourier Transform (FFT) method. The scheme is also capable of incorporating features such as a “reset provision”, which is a penalty structure used as a disincentive to excessive withdrawals.

Luo and Shevchenko (2014) develop a computationally efficient approach for pricing the GMWBs. They use higher order Gauss-Hermite quadrature to numerically integrate cubic spline interpolations. The algorithm can be used for both static and dynamic behaviour, but requires a known probability density function of asset returns.

Recent innovations include algorithms that introduce further levels of stochasticity in GMWB valuation frameworks. Ignatieva et al. (2016) apply a Fourier space time-stepping algorithm to value the GMWB contract under a GBM regime-switching framework, subject to stochastic mortality risk. The authors note that fees decrease with the force of interest. Gudkov et al. (2016) assume stochastic volatility, stochastic interest rates, and stochastic mortality. The first two are found to have significant influence on the resulting fair fees while the impact of mortality on the fair fee is small.

Moenig and Bauer (2016) take a deeper look into the optimal decisions made by policyholders by considering the impact of tax benefits on withdrawal behaviour. When accounting for such benefits, they find that dynamic policyholder fair fees in the GBM framework are in line with fees observed in the market.

Hedging of VA guarantees has attracted substantial academic interest of late, with a particular focus on GMWBs. Coleman et al. (2007) use local risk minimisation strategies to hedge guaranteed minimum death benefits. Kolkiewicz and Liu (2012) take a similar approach to Coleman et al. (2007), but instead hedge GMWBs. The authors show that under the Black and Scholes (1973) framework, delta-gamma hedging outperforms the risk minimisation strategies only if the withdrawals are very frequent. However, when jumps are introduced into the asset dynamics, hedging the Greeks is ineffective, whereas the risk minimisation strategies perform well. Bernard and Kwak (2016) extend the Coleman et al. (2007) hedging strategy by showing that the insurer can use the periodic fees received to improve the performance of a hedging strategy.

Other strategies have also been considered, such as Goudenege et al. (2016), who hedge the Greeks of a GMWB rider under both the Hull and White (1990) stochastic interest rate model and the Heston (1993) stochastic volatility model. Ignatieva et al. (2016) also hedge the Greeks in their regime-switching framework with an additional focus of hedging mortality risk. Carr et al. (2016) perform a case study analysis of hedging the net present value of future cash flows of a GMWB portfolio using a transformed multivariate normal distribution fitted to nine indices. Feng and Vecer (2016) perform an analysis on risk capital by formulating the profit-loss distribution of GMWBs using PDE methods.

In this paper we value the GMWB rider with the aid of the COS method. The COS method is first presented in Fang and Oosterlee (2008) as an efficient numerical integration method for pricing European-style options. A follow up paper showing how the method can be used to pricing early-exercise options, such as the Bermudan option, is presented in Fang and Oosterlee (2009). The two studies demonstrate the comparative efficiency of the COS method with existing efficient numerical derivative pricing techniques, such as the convolutions (CONV) method (Lord et al., 2008). Furthermore, the authors validate the robustness of the COS method through accurate pricing of the derivatives when modelling assets driven by infinite activity Lévy processes, such as CGMY, and the Heston (1993) stochastic volatility model.

Further uses of the COS method include pricing derivatives with multiple underlying assets (Ruijter and Oosterlee, 2012), applying it to stochastic optimal control problems (Ruijter et al., 2013), pricing equity-indexed life annuities (Deng et al., 2015), and for use in ruin theory applications (Chau et al., 2015a,b).

In this paper, we provide an efficient algorithm for pricing VAs embedded with GMWB riders using the COS method. Unlike the algorithm in Luo and Shevchenko (2014), the density function does not need to be known in closed form. We then use the framework to further investigate the use of risk minimisation hedging strategies, using concepts outlined in Kolkiewicz and Liu (2012).

The algorithm we develop demonstrates superior computational efficiency as it can be adapted to the general class of Lévy processes. These processes are general enough to include a wealth of patterns and thus they account for the smile and skew effects observed in option prices (Papantoleon, 2008). We also extend the use of the COS method to develop hedging strategies that seek to minimise a moment or quantile-based risk measure, such as the variance of the hedging outcomes or the 95% Value at Risk (VaR) of the hedged portfolio loss distribution. We show that the COS method is computationally more efficient in comparison with valuation methodologies in existing literature for the same level of accuracy. The framework developed is general enough to incorporate complex policyholder behavior decisions and sophisticated contract features such as the reset provision. The local risk minimization strategies developed can incorporate short-selling and budgeting constraints while remaining robust. The framework developed proves to be compatible to both pricing, delta-gamma hedging, risk minimization and VaR calculations, making it a strong candidate for quick and accurate valuations for the industry.

The remainder of the paper is structured as follows. In Section 2 we first describe the asset and account dynamics, and then continue to formulate the pricing problem and explain the use of the COS method. Section 3 outlines the hedging framework, describing the local risk minimisation problem as well as how the Greeks are hedged, and again explaining the use of the COS method. Numerical results and analysis of the framework are presented in Section 4 before the paper is concluded in Section 5.

2 GMWB Valuation Framework

2.1 Asset Dynamics

Lévy processes incorporate a large number of well known models, such as the GBM (Black and Scholes, 1973), Variance Gamma (VG) (Madan and Seneta, 1990) and Carr Geman Madan Yor (CGMY) models (Carr et al., 2002). Lévy processes may be defined in terms of their *Lévy triplet*, (μ, σ^2, ν) , which fully specifies the process through its drift term, μ , diffusion coefficient, σ , and *Lévy measure*, ν . The Lévy measure, intuitively, is the expected number of jumps of a specific magnitude in a time interval of one (Papantoleon, 2008). The general dynamics of a Lévy process with triplet (μ, σ^2, ν) are then given by

$$dL_t = \mu dt + \sigma dW_t + d\tilde{M}_t, \quad (2.1)$$

where W_t is a standard Brownian motion under the real measure P and \tilde{M}_t is a compensated compound Poisson process. These processes are linked to their probability distributions through the Lévy-Khintchine formula, which expresses the characteristic function of a Lévy process with triplet (μ, σ^2, ν) as follows

$$\phi(u) = \exp \left[i\mu u - \frac{u^2 \sigma^2}{2} + \int_{\mathbb{R}} (e^{iux} - 1 - iux \mathbf{1}_{\{|x| < 1\}}) \nu(dx) \right]. \quad (2.2)$$

Analogous to the frequently used GBM, when using Lévy processes in finance we model asset prices with an *exponential* Lévy process. Thus, denoting S_t as the asset price process, and using

a Lévy process that satisfies Equation (2.1) we have

$$S_t = S_0 e^{L_t},$$

where L_t is a Lévy process with triplet (μ, σ^2, ν) . This model shares some essential properties with the GBM for pricing derivatives. Such properties include being bounded below by zero, and having independent, stationary increments of the log-asset returns. Lévy processes are general enough to include a wealth of patterns and thus they account for the smile and skew effects observed in option prices (Papapantoleon, 2008). The general dynamics of an underlying asset influenced by exponential Lévy processes, with Lévy triplet (μ, σ^2, ν) , can be represented as

$$dS_t = S_t \left(dL_t + \frac{\sigma^2}{2} dt + \int_{\mathbb{R}} (e^x - 1 - x) N(dt, dx) \right), \quad (2.3)$$

where dL_t is defined in Equation (2.1) (Papapantoleon, 2008). The risk-neutral dynamics of the underlying asset are given by substituting dL_t in Equation (2.3) with $dL_t^{\mathbb{Q}}$, where $L_t^{\mathbb{Q}}$ is a Lévy process with a risk-neutral Brownian motion, $W_t^{\mathbb{Q}}$, and triplet

$$\left(r - \frac{\sigma^2}{2} - \int_{\mathbb{R}} (e^x - 1 - x) \nu(dx), \sigma^2, \nu \right), \quad (2.4)$$

such that $S_t e^{-rt}$ is a martingale under the risk-neutral measure. See Appendix A.1 for detail about the solution to the integral component of the triplet in Equation (2.4).

2.2 The Variable Annuity Account Dynamics

In order to make direct comparisons to existing literature, we primarily adopt the variable annuity account dynamics presented in Luo and Shevchenko (2014). Changes can also be made to the framework in order to compare with Bacinello et al. (2014) in the static case.

The VA contract with an embedded GMWB rider provides the policyholder with two accounts, namely an investment account and a guarantee account which guarantees the return of the policyholder's initial premium A_0 over the term of the contract. This is achieved by guaranteeing a withdrawal of $G = \frac{A_0}{M}$ at each of the M withdrawal dates, where G is called the *guaranteed rate*. Both the investment account, W_t , and guarantee account, A_t , are bounded below by zero. The two accounts start with a value of W_0 , which corresponds to the VA's initial premium. The investment account accumulates according to the dynamics of S_t , described in Equation (2.3). However, at withdrawal dates, denoted here as t_m (for $m = 1, \dots, M$), with t_M corresponding to the maturity of the contract, both W_{t_m} and A_{t_m} drop instantaneously by the withdrawal amount γ_{t_m} . Additionally, an insurance fee of $\alpha\%$ p.a. is deducted from the investment account continuously. If W_t hits zero before maturity of the contract, withdrawals will continue to be made until the entire guarantee account is depleted.

To avoid confusion about the exact timing of withdrawals and valuations, we adopt the following notation:

- t_m^- is the instant before the m^{th} withdrawal date;
- t_m is the exact moment at which a withdrawal occurs; and
- t_m^+ is the instant after the m^{th} withdrawal date.

This notation is graphically represented in Figure 1, which shows the m^{th} withdrawal date being expanded into the three times, t_m^- , t_m and t_m^+ . Each of the M withdrawal dates is split up in the same way.

To illustrate how this notation is utilised, consider Figure 2, which shows an example path of the GMWB investment and guarantee accounts. In this figure, t_m corresponds to times 1, 2, 3, 4 and 5.

Figure 1: Time index for the M withdrawal dates.

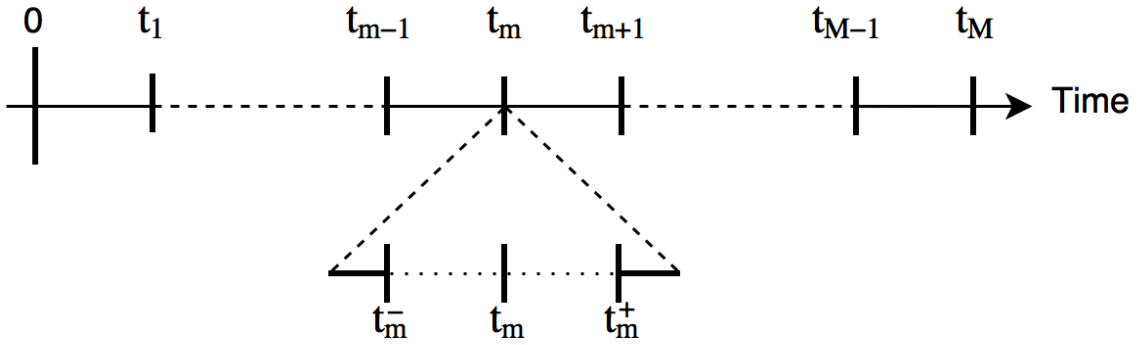
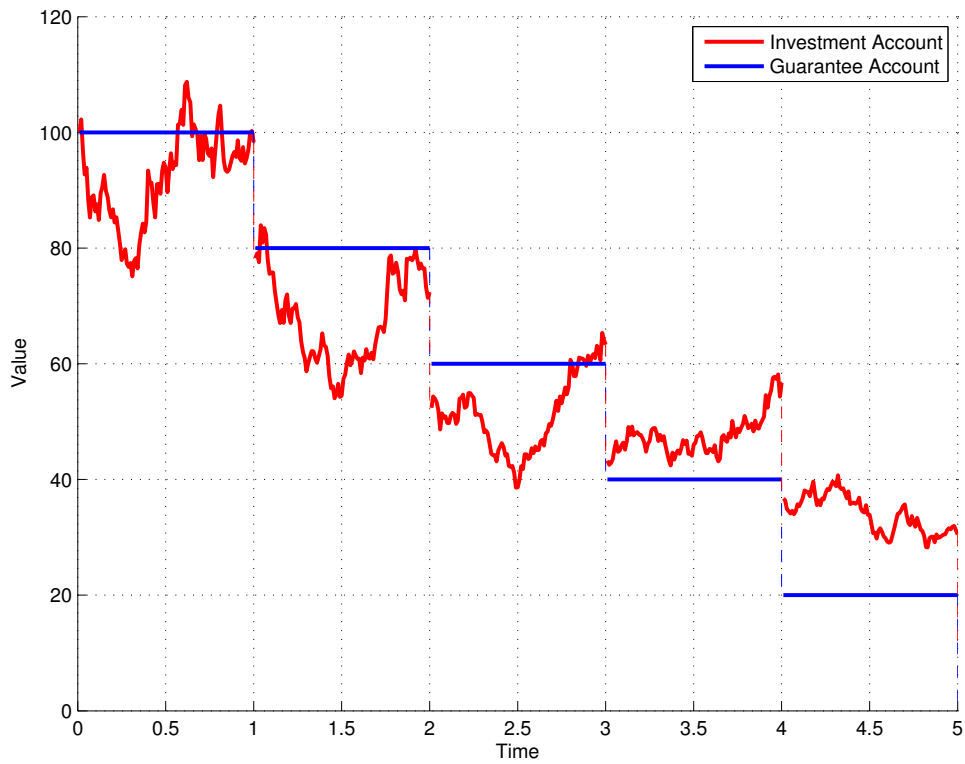


Figure 2: Example path of the investment and guarantee accounts for a five-year GMWB.



Note that the guarantee account remains unchanged between withdrawal dates, as shown in Figure 2. Mathematically, the guarantee account evolves as follows:

$$A_{t_m^+} = A_{t_{m+1}^-} = \max \left[A_{t_m^-} - \gamma_{t_m}, 0 \right], \quad (2.5)$$

where γ_{t_m} is the withdrawal amount decided upon by the policyholder at withdrawal time t_m . The withdrawal amount can be either deterministic and pre-specified in the contract or a \mathcal{F}_{t_m} measurable random variable, where \mathcal{F}_{t_m} corresponds to the filtration at time t_m . When incorporating the reset provision¹, the guarantee account instead evolves according to the following formula:

$$A_{t_m^+} = A_{t_{m+1}^-} = \begin{cases} \max \left[A_{t_m^-} - \gamma_{t_m}, 0 \right], & \text{if } \gamma_{t_m} \leq G \\ \max \left[\min \left[A_{t_m^-} - \gamma_{t_m}, W_{t_m^-} - \gamma_{t_m} \right], 0 \right], & \text{if } \gamma_{t_m} > G. \end{cases}$$

The investment account, under the risk-neutral dynamics, evolves according to:

$$\begin{aligned} W_{t_{m+1}^-} &= \max \left[\left(W_{t_m^-} - \gamma_{t_m} \right), 0 \right] \cdot \exp \left[L_{t_{m+1}-t_m}^{\mathbb{Q}} \right] \cdot \exp \left[-\alpha (t_{m+1} - t_m) \right] \\ &= \max \left[W_{t_m^+}, 0 \right] \cdot \exp \left[L_{t_{m+1}-t_m}^{\mathbb{Q}} \right] \cdot \exp \left[-\alpha (t_{m+1} - t_m) \right], \end{aligned} \quad (2.6)$$

where $W_{t_m^+} = \left(W_{t_m^-} - \gamma_{t_m} \right)$, as highlighted in Figure 2. For comparison to Bacinello et al. (2014) and for use in the hedging framework, the insurance fee will be deducted discretely at withdrawal dates. In this case the investment account evolves as follows

$$W_{t_{m+1}^-} = \max \left[W_{t_m^+} (1 - \alpha(t_{m+1} - t_m)), 0 \right] \cdot \exp \left[L_{t_{m+1}-t_m}^{\mathbb{Q}} \right].$$

Withdrawals above the guaranteed rate are subject to a proportional penalty fee, κ . Thus, the cash flows actually received by the policyholder can be represented as

$$C(\gamma_{t_m}) = \begin{cases} \gamma_{t_m} & \text{if } 0 \leq \gamma_{t_m} \leq G, \\ G + (1 - \kappa) \cdot (\gamma_{t_m} - G) & \text{if } \gamma_{t_m} > G. \end{cases}$$

The discounted risk-neutral valuation of the contract at time t_m , given the time t_m^- value of the guarantee and investment accounts, may be found by solving the following equation

$$\begin{aligned} V_{t_m}(W_{t_m^-}, A_{t_m^-}) &= \sup_{\gamma} \left[\mathbb{E}^{\mathbb{Q}} \left[e^{-r(T-t_m)} \max[W_{t_M}, C(A_{t_M})] \right. \right. \\ &\quad \left. \left. + \sum_{j=m}^{M-1} e^{-r(t_j-t_m)} C(\gamma_{t_j}) \middle| W_{t_m^-}, A_{t_m^-}, \gamma_{t_m} \right] \right], \end{aligned} \quad (2.7)$$

where γ is defined in the interval $[0, \dots, 0, A_{t_m^-}]$. The equation (2.7) effectively represents the risk-neutral expected present value of all future cash flows. The first term within the expectation in Equation (2.7) implies that the terminal condition of the contract is

$$V_{t_M}(W_{t_M}, A_{t_M}) = \max[W_{t_M}, C(A_{t_M})]. \quad (2.8)$$

The supremum term in Equation (2.7) emulates rational withdrawal behaviour. However, withdrawals can be made either statically or dynamically. To differentiate between the static and dynamic policyholder behaviour types, we restrict the values that γ_{t_m} can take as follows:

$$\gamma_{t_m} \in \begin{cases} \{G\}, & \text{in the static case; and} \\ \left[0, A_{t_m^-} \right], & \text{in the dynamic case.} \end{cases} \quad (2.9)$$

¹Reset provisions are a form of penalty that potentially ‘resets’ the guarantee account, following a withdrawal above the guaranteed rate, to the minimum of the investment and guarantee account values (Chen et al., 2008).

2.3 The COS Method

2.3.1 Derivations

The COS method, as presented in Fang and Oosterlee (2008), relies on Fourier-cosine series expansions. Any finite function, $f(\cdot)$, on $[0, \pi]$ can be expressed in terms of its Fourier-cosine expansion

$$f(\theta) = \sum_{k=0}^{\infty} 'A_k \cdot \cos(k\theta), \text{ with } A_k = \frac{2}{\pi} \int_0^{\pi} f(\theta) \cos(k\theta) d\theta,$$

where the apostrophe denotes that the first term in the summation is halved. Thus, by performing the following change of variable:

$$\theta = \frac{y-a}{b-a}\pi; \quad y = \frac{b-a}{\pi}\theta + a,$$

the function $f(\cdot)$ on the interval $[a, b]$ can be expanded as follows

$$f(y) = \sum_{k=0}^{\infty} 'A_k \cdot \cos\left(k\pi \frac{y-a}{b-a}\right), \text{ with } A_k = \frac{2}{b-a} \int_a^b f(y) \cos\left(k\pi \frac{y-a}{b-a}\right) dy.$$

The coefficient term, A_k , can be re-expressed as an exponential term by recalling that $\exp(i\omega) = \cos(\omega) + i \sin(\omega)$, such that

$$A_k = \frac{2}{b-a} \operatorname{Re} \left\{ \int_a^b f(y) \cdot \exp\left(ik\pi \frac{y-a}{b-a}\right) dy \right\},$$

where $\operatorname{Re}\{\cdot\}$ is the real part of a value and $i = \sqrt{-1}$ is the imaginary unit. We define $\psi_1(\cdot)$, a truncated version of the characteristic function $\psi(\cdot)$, such that

$$\phi_1(\omega) = \int_a^b e^{ix\omega} f(x) dx \approx \int_{\mathbb{R}} e^{ix\omega} f(x) dx = \phi(\omega).$$

Using the results above, a density function can be approximated in terms of its characteristic function via

$$\begin{aligned} f(y) &= \frac{2}{b-a} \sum_{k=0}^{\infty} ' \operatorname{Re} \left\{ \phi_1\left(\frac{k\pi}{b-a}\right) \cdot \exp\left(-i \frac{ka\pi}{b-a}\right) \right\} \cos\left(k\pi \frac{y-a}{b-a}\right) \\ &\approx \frac{2}{b-a} \sum_{k=0}^{N-1} ' \operatorname{Re} \left\{ \phi\left(\frac{k\pi}{b-a}\right) \cdot \exp\left(-i \frac{ka\pi}{b-a}\right) \right\} \cos\left(k\pi \frac{y-a}{b-a}\right), \end{aligned} \quad (2.10)$$

where the approximation arises from truncating the infinite series to N terms, and by approximating $\phi_1(\cdot)$ with the actual characteristic function, $\phi(\cdot)$.

Making use of the following result for the conditional characteristic functions of Lévy processes

$$\phi(\omega; x) = \phi(\omega) \cdot e^{i\omega x},$$

it is also easy to approximate conditional density functions using the following formula

$$\begin{aligned} f(y|x) &= \frac{2}{b-a} \sum_{k=0}^{\infty} ' \operatorname{Re} \left\{ \phi_1\left(\frac{k\pi}{b-a}; x\right) \cdot \exp\left(-i \frac{ka\pi}{b-a}\right) \right\} \cos\left(k\pi \frac{y-a}{b-a}\right) \\ &\approx \frac{2}{b-a} \sum_{k=0}^{N-1} ' \operatorname{Re} \left\{ \phi\left(\frac{k\pi}{b-a}\right) \cdot \exp\left(ik\pi \frac{x-a}{b-a}\right) \right\} \cos\left(k\pi \frac{y-a}{b-a}\right). \end{aligned} \quad (2.11)$$

Fang and Oosterlee (2008) recommend selecting the truncation range, $[a, b]$, based on the i^{th} cumulants, c_i , of the underlying density function, such that

$$[a, b] = \left[c_1 - L\sqrt{c_2 + \sqrt{c_4}}, c_1 + L\sqrt{c_2 + \sqrt{c_4}} \right], \quad (2.12)$$

where L is a constant chosen to cover the desired portion of the density function. Refer to Appendix A.2 for the relevant cumulants.

2.3.2 Numerical Implementation

The value of the GMWB contract is found by implementing a backward recursive algorithm, subject to the terminal condition in Equation (2.8). The backward recursion approach to this type of optimal control problem relies on the dynamic programming principle, which essentially says that the decision choice at a particular time will not affect previous optimal decisions (Ruijter et al., 2013). The significance of this is that the optimal withdrawal at time t_m only depends on the investment and guarantee account values and the time, but is not affected by withdrawal decisions made at time t_n , for $n < m$.

By rearranging Equation (2.7), the valuation problem can be expressed recursively as

$$\begin{aligned} V_{t_m} \left(W_{t_m}^-, A_{t_m}^- \right) &= \sup_{\gamma} \left[\mathbb{E}^{\mathbb{Q}} \left[C(\gamma_{t_m}) + e^{-r(t_{m+1}-t_m)} V_{t_{m+1}} \left(W_{t_{m+1}}^-, A_{t_{m+1}}^-; \gamma_{t_m} \right) \middle| W_{t_m}^-, A_{t_m}^-, \gamma_{t_m} \right] \right] \\ &= \sup_{\gamma} \left[C(\gamma_{t_m}) + e^{-r(t_{m+1}-t_m)} \underbrace{\mathbb{E}^{\mathbb{Q}} \left[V_{t_{m+1}} \left(W_{t_{m+1}}^-, A_{t_{m+1}}^-; \gamma_{t_m} \right) \middle| W_{t_m}^-, A_{t_m}^-, \gamma_{t_m} \right]}_{\zeta} \right]. \end{aligned} \quad (2.13)$$

The risk-neutral expectation term, denoted ζ in Equation (2.13), is approximated using the COS method (Fang and Oosterlee, 2008).

The first step is to explicitly write ζ in integral form,

$$\begin{aligned} \zeta &= \mathbb{E}^{\mathbb{Q}} \left[V_{t_{m+1}} \left(W_{t_{m+1}}^-, A_{t_{m+1}}^-; \gamma_{t_m} \right) \middle| W_{t_m}^-, A_{t_m}^-, \gamma_{t_m} \right] \\ &= \int_{-\infty}^{\infty} V_{t_{m+1}} \left(w_{t_{m+1}}^-, A_{t_{m+1}}^-; \gamma_{t_m} \right) g^{\mathbb{Q}}(w_{t_{m+1}}^- | W_{t_m}^-, \gamma_{t_m}) dw_{t_{m+1}}^-, \end{aligned} \quad (2.14)$$

where $g^{\mathbb{Q}}(\cdot)$ is the risk-neutral conditional probability density function of the investment account value at the next withdrawal date, $W_{t_{m+1}}^-$.

It is then possible to perform a change of variable, such that the integral is re-expressed in terms of the underlying stock's² one-period return, $y = \ln \left(\frac{S_{t_{m+1}}}{S_{t_m}} \right)$. The risk-neutral distribution of the stock return is assumed to have a Lévy distribution, and thus its characteristic function is known. The distribution between each withdrawal date is identically and independently distributed due to the Lévy properties. Recall that $W_{t_{m+1}}^- = \max \left[W_{t_m}^+, 0 \right] \cdot \exp \left[L_{t_{m+1}-t_m}^{\mathbb{Q}} \right]$ and $A_{t_{m+1}}^- = A_{t_m}^- - \gamma_{t_m}$, so that Equation (2.14) becomes

$$\zeta = \int_{-\infty}^{\infty} V_{t_{m+1}} \left(\max \left[W_{t_m}^+, 0 \right] \cdot e^y, A_{t_m}^+; \gamma_{t_m} \right) f^{\mathbb{Q}}(y) dy,$$

²We will use 'asset' or 'stock' to mean the same thing. Therefore these two words will be used interchangeably.

where $f^{\mathbb{Q}}(\cdot)$ is the risk-neutral probability density function of the one-period stock return, which follows a Lévy distribution. We then approximate ζ with ζ_1 by truncating the integration range to $[a, b]$, such that

$$\zeta \approx \zeta_1 = \int_a^b V_{t_{m+1}} \left(\max \left[W_{t_m^+}, 0 \right] \cdot e^y, A_{t_m^+}; \gamma_{t_m} \right) f^{\mathbb{Q}}(y) dy, \quad (2.15)$$

where a and b are calculated using Equation (2.12).

We expand the risk-neutral density function using the unconditional form of its COS approximation, Equation (2.10). Recall that the approximation involves truncating the Fourier-cosine series to N terms and approximating $\phi_1(\cdot)$ with $\phi(\cdot)$. This results in the subsequent approximation

$$\begin{aligned} \zeta_1 \approx \zeta_2 &= \int_a^b V_{t_{m+1}} \left(\max \left[W_{t_m^+}, 0 \right] \cdot e^y, A_{t_m^+}; \gamma_{t_m} \right) \\ &\quad \times \frac{2}{b-a} \sum_{k=0}^{N-1} \text{Re} \left\{ \phi^{\mathbb{Q}} \left(\frac{k\pi}{b-a} \right) \cdot \exp \left(-i \frac{ka\pi}{b-a} \right) \right\} \cos \left(k\pi \frac{y-a}{b-a} \right) dy, \end{aligned}$$

where $\phi^{\mathbb{Q}}(\cdot)$ is the risk-neutral characteristic function corresponding to the one-period stock return distribution. Now the components of ζ_2 that are not functions of y are rearranged outside of the integral. The final formula used for approximating ζ is

$$\zeta \approx \zeta_2 = \sum_{k=0}^{N-1} \text{Re} \left\{ \phi^{\mathbb{Q}} \left(\frac{k\pi}{b-a} \right) \cdot \exp \left(-i \frac{ka\pi}{b-a} \right) \right\} \cdot U_k \left(W_{t_m^+}, A_{t_m^+} \right), \quad (2.16)$$

where

$$U_k \left(W_{t_m^+}, A_{t_m^+} \right) = \frac{2}{b-a} \int_a^b V_{t_{m+1}} \left(\max \left[W_{t_m^+}, 0 \right] \cdot e^y, A_{t_m^+}; \gamma_{t_m} \right) \cdot \cos \left(k\pi \frac{y-a}{b-a} \right) dy. \quad (2.17)$$

Since the terminal condition, Equation (2.8), is known in closed-form, a backwards recursion can be set up to extract the time zero value of the contract.

The terminal condition means that the U_k coefficients at the maturity time-step can be expressed in terms of analytically known functions $\psi_k(\cdot, \cdot)$ and $\chi_k(\cdot, \cdot)$

$$\begin{aligned} U_k(W_{t_{M-1}^+}, A_{t_{M-1}^+}) &= \frac{2}{b-a} \int_a^b V_{t_M} \left(\max \left[W_{t_{M-1}^+}, 0 \right] \cdot e^y, A_{t_{M-1}^+}; \gamma_{t_{M-1}} \right) \cdot \cos \left(k\pi \frac{y-a}{b-a} \right) dy \\ &= \frac{2}{b-a} \int_a^{y^*} A_{t_{M-1}^+} \cdot \cos \left(k\pi \frac{y-a}{b-a} \right) dy \\ &\quad + \frac{2}{b-a} \int_{y^*}^b W_{t_{M-1}^+} \cdot e^y \cdot \cos \left(k\pi \frac{y-a}{b-a} \right) dy \\ &= \frac{2}{b-a} \left(A_{t_{M-1}^+} \cdot \psi_k(a, y^*) + W_{t_{M-1}^+} \cdot \chi_k(y^*, b) \right), \end{aligned} \quad (2.18)$$

$$\text{where } y^* = \min \left[\max \left[\ln \left(\frac{A_{t_{M-1}^+}}{\max \left[W_{t_{M-1}^+}, 0 \right]} \right), a \right], b \right], \quad (2.19)$$

with $\psi_k(\cdot, \cdot)$ and $\chi_k(\cdot, \cdot)$ as defined in Appendix B. This definition of y^* ensures that each of the split integrals is still within the range $[a, b]$. Also note that y^* is well defined, regardless of the account values being zero, by considering the following cases:

- $\max \left[W_{t_{M-1}^+}, 0 \right] = 0 \rightarrow \min[\ln(\infty), b] = b$;
- $A_{t_{M-1}^+} = 0 \rightarrow \max[\ln(0), a] = a$; and
- $\max \left[W_{t_{M-1}^+}, 0 \right] = A_{t_{M-1}^+} = 0 \rightarrow \zeta = 0 \rightarrow$ integral calculation is unnecessary.

At other withdrawal times, the U_k coefficients are approximated numerically. Bringing this back to the pricing formula, the value of the GMWB at time t_m can be found recursively for different values of $W_{t_m^-}$ and $A_{t_m^-}$ as

$$V_{t_m} \left(W_{t_m^-}, A_{t_m^-} \right) = \sup_{\gamma} \left[C(\gamma_{t_m}) + e^{-r(t_{m+1}-t_m)} \sum_{k=0}^{N-1} \text{Re} \left\{ \phi^{\mathbb{Q}} \left(\frac{k\pi}{b-a} \right) e^{\frac{-ika\pi}{b-a}} \right\} \cdot U_k \left(W_{t_m^+}, A_{t_m^+} \right) \right]. \quad (2.20)$$

Due to the complex nature of this contract, particularly in the dynamic withdrawals case, the fair insurance fee cannot be found analytically. Instead, the bisection method is used to find the fair fee. This involves multiple iterations of calculating the GMWB's time zero value for different insurance fees until the value converges to W_0 . Since the initial value of a vanilla VA contract is simply the premium paid, the fair fee for the GMWB will be determined as the fee resulting in an unchanged initial value of the VA contract. The algorithm requires discretisation of the A and W account values at each time step, thus adding an aspect of approximation. Furthermore, the supremum term for γ must be approximated at each time step by considering a selection of discrete points, rather than every possible value. Please refer to Appendix C for further detail on the valuation algorithm for the static and dynamic case.

3 GMWB Hedging Strategies

Hedging can be performed with a wide variety of strategies. The portfolio manager has many considerations, such as which uncertainty to hedge, how frequently to rebalance portfolios, how the hedge is funded and the risk measures to consider. Hedging the Greeks, such as delta and gamma, is a popular hedging strategy, but is known to only be entirely effective in complete markets and when continuous portfolio rebalancing is possible (Derman et al., 1998). In practice, transaction costs limit the portfolio rebalancing to discrete intervals, which introduces a hedging error. Static hedges may be used to remove all risk from some derivative products if the hedging portfolio is held until maturity. However, it is still impossible to perfectly hedge GMWBs, due to a basis risk between the required hedges and the available hedging assets (Blamont and Sagoo, 2009). A major cause of this is a mismatch between the time to maturity of GMWBs and that of actively traded derivative products.

We compare several possible hedging strategies under different assumptions and constraints. Aside from the well known delta and delta-gamma hedging strategies, we also consider several risk minimisation hedging strategies. These are strategies that seek to minimise a chosen risk measure, generally based on real-world probabilities. We investigate risk minimisation strategies that are either based on minimising the moments of the hedging outcomes, such as variance, or based on the quantiles of the hedged portfolio loss distribution, such as minimising the portfolio 95% value-at-risk (VaR).

Upon maturity of a hedging position, either when the next set of hedging trades is made, or at maturity of the derivative to be hedged, the insurer will experience a hedging error. This could result in a loss or gain for the insurer. The performance of a hedging position can be determined based on its hedging error. The outcome of the hedge is unknown when selecting

the portfolio. Therefore, it is essential to consider the distribution of possible hedging errors. We assume that the insurer is more concerned with minimising potential hedging losses, as opposed to maximising potential gains. A perfect hedge would have zero hedging error regardless of the realised stock return, and a bad hedge would cause unfavourable changes to the distribution, such as increasing the likelihood of making a hedging loss and increasing the variance of the hedging error. The remainder of this section outlines the techniques used to select GMWB hedging portfolios.

3.1 Assumptions

Coleman et al. (2007) find that risk minimisation hedging can be much more effective with the use of European options, rather than the underlying asset. For our analysis we assume that there are actively traded derivatives on the asset underlying the VA from which a hedging portfolio can be constructed with no transaction costs. Furthermore, it is assumed that the derivatives can be purchased at the withdrawal dates such that they mature on the next withdrawal date. Hedge portfolio rebalancing will occur only on withdrawal dates.

A common assumption in hedging theory is that short-selling of derivatives is allowed. In fact, it is not always the case that insurers are allowed to short-sell derivatives (ASIC, 2012). Any constraint on the amount of trading allowed can be factored into the portfolio selection process. We consider each of the cases where short-selling is allowed, where short-selling is not allowed, and when short-selling is limited. For hedging the Greeks, it is assumed that short-selling is allowed, and that the underlying asset and a risk-free asset are also available for trading.

Another consideration is the budgeting constraint of the insurer. It may be that the insurer wishes to allocate a certain proportion of the fees received from the GMWB contract to fund the hedging portfolio. Funds are also generated through short-selling, subject to constraints. Once again, it is easy to account for a diverse range of budgeting constraints.

3.2 Risk Minimisation Strategies

The approach for risk minimisation strategies is based on the strategy presented in Kolkiewicz and Liu (2012). This method involves selecting an optimal portfolio of vanilla European options to hedge GMWB contracts, by minimising the second moment of the hedging error. As an example, the authors define the hedging error as the change in net liability of the hedged portfolio at the next time period. In general this could be any uncertain value that is to be hedged and that is dependent on the underlying asset. Although other assumptions can be used, risk minimisation strategies generally act on real-world probabilities. The general structure of the approach used to determine the hedging portfolio is outlined below.

Suppose that we want to hedge some uncertainty at time t_{m+1} , that is dependent on the underlying asset value, denoted $H_{t_{m+1}}(S_{t_{m+1}}|S_{t_m}, V_{t_m}(W_{t_m}^+))$, with information of the time t_m^+ values of the stock and GMWB contract, by constructing a hedging portfolio of European options with the same underlying asset as the GMWB. The hedging portfolio will be determined such that a chosen risk measure, $\rho(\cdot)$, is minimised resulting in the hedged uncertainty, $H_{t_{m+1}}^\rho(S_{t_{m+1}}|S_{t_m}, V_{t_m}(W_{t_m}^+), \vec{\theta})$.

Defining the payoff function of the j^{th} option, which can be a European put or call that matures at time t_{m+1} , as $F(S_{t_{m+1}}, K_j)$, the hedging error of the hedged portfolio with n different options is

$$H_{t_{m+1}}^\rho \left(S_{t_{m+1}} \middle| S_{t_m}, V_{t_m} \left(W_{t_m}^+ \right), \vec{\theta} \right) = H_{t_{m+1}} \left(S_{t_{m+1}} \middle| S_{t_m}, V_{t_m} \left(W_{t_m}^+ \right) \right) - \sum_{j=1}^n \theta_j \cdot F \left(S_{t_{m+1}}, K_j \right),$$

where θ_j is the amount of the j^{th} option purchased. The optimal hedging portfolio, $\vec{\theta}^\rho$, is determined by solving the following optimisation problem

$$\vec{\theta}^\rho = \inf_{\vec{\theta}} \left[\rho \left(H_{t_{m+1}}^\rho \left(S_{t_{m+1}} \left| V_{t_m} \left(W_{t_m}^+ \right), S_{t_m}, \vec{\theta} \right) \right) \right) \right],$$

where $S_{t_{m+1}} = S_{t_m} \cdot e^y$, and the infimum is found subject to the various assumptions and constraints discussed in Subsection 3.1. The unhedged and hedged portfolios will be referred to as $H(y)$ and $H^\rho(y|\vec{\theta})$, respectively, for notational convenience. We investigate the effectiveness of hedging with several risk measures. The approach is separated into risk measures that are based on the moments of the hedging loss distribution, and those that are based on the quantiles of the distribution, such as the VaR.

All information that might be required in the hedging process can be extracted from the valuation framework by valuing at some withdrawal date, t_m , instead of at time zero. If necessary, the valuation framework can output the time t_m valuation and withdrawal decision, as well as the vectors of time t_{m+1} valuations and withdrawal decisions.

3.2.1 Moment-Based Risk Measures

Moments of the hedging error can be easily approximated using the COS method. Essentially, the only difference to Equation (2.16), which is the COS approximation of ζ , is that we are looking at the value of the whole portfolio, and that instead of only looking at the first moment (i.e. the expected value), we are approximating

$$E \left[\left(H^\rho \left(Y | \vec{\theta} \right) \right)^n \right] = \int_{-\infty}^{\infty} \left(H^\rho \left(y | \vec{\theta} \right) \right)^n \cdot f(y) dy, \quad (3.1)$$

for any $n = \{1, 2, \dots\}$, where Y is the random distribution of possible one-period stock returns. Note that $f(\cdot)$ represents the real-world probability density function of the one-period stock return. Equation (3.1) can be approximated using the COS method, as in Subsection 2.3, such that

$$E \left[\left(H^\rho \left(Y | \vec{\theta} \right) \right)^n \right] \approx \sum_{k=0}^{N-1} \text{Re} \left\{ \phi \left(\frac{k\pi}{b-a} \right) e^{\frac{-ika\pi}{b-a}} \right\} \cdot U_k \left(W_{t_m}^+, A_{t_m}^+ | \vec{\theta} \right), \quad (3.2)$$

where

$$U_k \left(W_{t_m}^+, A_{t_m}^+ | \vec{\theta} \right) = \frac{2}{b-a} \int_a^b \left(H_{t_{m+1}}^\rho \left(y | \vec{\theta} \right) \right)^n \cdot \cos \left(k\pi \frac{y-a}{b-a} \right) dy.$$

It follows that this can be applied to compute any moments-based risk measure, such as the example of hedging the second moment provided in Kolkiewicz and Liu (2012).

3.2.2 Quantile-Based Risk Measures

The interest in quantile-based risk measures comes mainly from the VaR and tail value-at-risk (TVaR) values of the hedging error distribution. A $q\%$ VaR represents the q^{th} quantile of a loss distribution, while the $q\%$ TVaR measure is the expected loss given that the loss is larger than the $q\%$ VaR. This information is particularly important for regulatory purposes, where insurers are often required to hold enough capital to withstand, for example, a one in two hundred year loss (Dhaene et al., 2003).

In this context, the loss we are interested in is the level of hedging error. Since the values of the hedging portfolio are known for many different realisations of the stock return, y , we are able to approximate the distribution of the hedging error.

First, the density of each y is calculated using Equation (2.10), the COS method probability density approximation. Thus, the density for the hedging error corresponding to each y at which the GMWB has been valued at time t_{m+1} can be approximated, since $f^h(H(y)) \propto f(y)$, where $f^h(\cdot)$ is the probability density function of the hedging loss distribution:

$$f^h\left(H\left(y^{(j)}\right)\right) \propto \sum_{\text{all } i} f\left(y^{(i)}\right) \cdot \mathbf{1}_{\{H(y^{(i)})=H(y^{(j)})\}},$$

Note that the summation and indicator function, $\mathbf{1}_{\{H(y^{(i)})=H(y^{(j)})\}}$, account for the case when multiple realisations of y lead to the same hedging loss.

Then, the hedging errors, corresponding to each y , are sorted into ascending order, with a loss being positive and a gain being negative. The q^{th} quantile is approximated by finding the hedging error below which $q\%$ of the distribution lies.

This method is utilised for hedging the VaR and TVaR risk measures. The $q\%$ VaR simply is the q^{th} quantile, whereas TVaR requires one further step. The $q\%$ TVaR is calculated as

$$TVaR_q\left(H^\rho\left(Y|\vec{\theta}\right)\right) \approx \frac{1}{1-q} \int_q^1 VaR_x\left(H^\rho\left(Y|\vec{\theta}\right)\right) f^{h^\rho}\left(VaR_x\left(H^\rho\left(Y|\vec{\theta}\right)\right)\right) dx,$$

which is evaluated using numerical integration.

3.3 Delta and Delta-Gamma Hedging

For hedging of the Greeks we consider delta and gamma. Recall that delta is the amount by which the financial derivative's value will change when a small shift in the underlying asset price occurs, and gamma is the amount by which the delta shifts in the same circumstance.

Delta (and delta-gamma) hedging strategies involve selecting a portfolio of hedging assets with the exact same delta (and gamma) values as the GMWB liability. This means that any small shift in the underlying asset value will cause the hedging assets and GMWB liability to move by the same amount, thus removing risk. We limit the number of portfolio rebalances to occur only at withdrawal dates, rather than continuous rebalancing, thus introducing a hedging error.

Taking the derivative of the GMWB value with respect to the underlying stock is not trivial in the COS valuation framework, due to the appearance of S_{t_m} in our definition of y , the inter-period asset return. Instead, we can approximate these values by looking at what happens to the value of the GMWB at time t_m if there is a small shift in the underlying asset's value at time t_m^+ . Note that the timing here is important, as the Greeks calculations should not impact the withdrawal decision made at time t_m . This shift will cause a proportional shift in the investment account value, $W_{t_m^+}$. The following are common finite differencing approximations for delta, Δ , and gamma, Γ , albeit applied to our notation, which consider a small shift, c , in the asset price

$$\Delta \approx \frac{V_{t_m}\left(W_{t_m^+} \cdot \frac{S_{t_m}+c}{S_{t_m}}\right) - V_{t_m}\left(W_{t_m^+}\right)}{c},$$

$$\Gamma \approx \frac{V_{t_m}\left(W_{t_m^+} \cdot \frac{S_{t_m}+c}{S_{t_m}}\right) - 2V_{t_m}\left(W_{t_m^+}\right) - V_{t_m}\left(W_{t_m^+} \cdot \frac{S_{t_m}-c}{S_{t_m}}\right)}{c^2}.$$

It is very easy to calculate these values using the valuation framework. The only change to Algorithm 1, in Appendix C, is that the returns required to reach known values at the next time-step are altered to account for the shift in $W_{t_m^+}$ caused by the shift in S_{t_m} . The next step is to match the calculated delta (and gamma) of the GMWB with the hedging assets.

3.3.1 European Options

The price of an option with payoff $F(S_{t_{m+1}}, K_j)$, denoted $v_{t_m}(S_{t_m}, K_j)$, must be known, if we are to be able to factor in budgeting constraints. In practice, this would be the market price. However, for this exercise the prices are found using the COS method. Furthermore, we also require the delta (and gamma) of the options in order to delta (and delta-gamma) hedge the GMWB contract. The flexibility of the COS method allows for these values to be approximated easily based on the characteristic function. Under the Black-Scholes framework these could instead be calculated analytically, but we choose not to for consistency in the approach. The formulae below are directly from Fang and Oosterlee (2008)

$$\begin{aligned} v_{t_m}(S_{t_m}, K_j) &\approx e^{-r(t_{m+1}-t_m)} \sum_{k=0}^{N-1} \text{Re} \left\{ \phi^{\mathbb{Q}} \left(\frac{k\pi}{b-a} \right) e^{ik\pi \frac{x-a}{b-a}} \right\} U_k, \\ \Delta &\approx e^{-r(t_{m+1}-t_m)} \sum_{k=0}^{N-1} \text{Re} \left\{ \phi^{\mathbb{Q}} \left(\frac{k\pi}{b-a} \right) e^{ik\pi \frac{x-a}{b-a}} \cdot \frac{ik\pi}{b-a} \right\} \frac{U_k}{S_{t_m}}, \\ \Gamma &\approx e^{-r(t_{m+1}-t_m)} \sum_{k=0}^{N-1} \text{Re} \left\{ \phi^{\mathbb{Q}} \left(\frac{k\pi}{b-a} \right) e^{ik\pi \frac{x-a}{b-a}} \cdot \left(\left(\frac{ik\pi}{b-a} \right)^2 - \frac{ik\pi}{b-a} \right) \right\} \frac{U_k}{S_{t_m}^2}. \end{aligned}$$

These formulae resemble Equation (2.16), but there are two important differences. Firstly, x here is defined as $\ln\left(\frac{S_t}{K}\right)$, and secondly, the U_k coefficients are known in closed form, that is

$$U_k = \begin{cases} K_j (\chi_k(0, b) - \psi_k(0, b)), & \text{for calls, and} \\ K_j (\psi_k(a, 0) - \chi_k(a, 0)), & \text{for puts,} \end{cases}$$

where the functions, $\chi(\cdot, \cdot)$ and $\psi(\cdot, \cdot)$, are defined in Appendix B. The flexibility of calculating these values with the COS method arises, once again, from requiring only the characteristic function of the stock return distribution.

The application of the valuation framework allows for a comprehensive framework with which the GMWB can be hedged. We can consider a wide spectrum of possible hedging strategies, such as local risk minimisation of moments-based and quantile-based risk measures, or hedging the Greeks. The framework also provides flexibility as to which uncertainty is hedged and for various constraints. Finally, using results from Fang and Oosterlee (2008), it is very easy to determine the price, delta, and gamma of European options, as well as the density of stock returns, provided the characteristic function of the asset returns is known.

4 Numerical Analysis

In this section we provide extensive analysis and discussion of the results obtained from numerical experiments for the valuation and hedging of VA contracts embedded with a GMWB rider. In Subsections 4.1 and 4.2 the efficiency of the model is assessed for both the static and dynamic policyholder withdrawal behaviour assumptions, respectively. Following the analysis of the valuation framework, Subsection 4.3 provides analysis of six scenarios to compare different hedging strategies.

To ensure that the model is working appropriately, we perform numerical comparisons with two existing valuation frameworks presented in Bacinello et al. (2014) and Luo and Shevchenko (2014). When valuing a VA contract with a GMWB rider, the fair fee is one that causes the time zero value of the contract to equal its initial premium, which we consider to be 100 units

in our numerical experiments. When comparing two numerical approximations to the problem, we do not expect convergence to exactly 100, but instead we aim for accuracy to several decimal places.

Throughout the analysis we consider three different asset return models which fall under the General Lévy framework for the sake of brevity. These are namely GBM, VG, and CGMY, whose characteristic functions are specified in Appendix A.1. Please note that our framework accommodates other General Lévy specifications. Primarily, we adopt the parameters presented in Bacinello et al. (2014), where the models have been calibrated to S&P 500 Option data. The fitted parameters are presented in Table 1.

Table 1: Bacinello et al. (2014) fitted model parameters.

Model	GBM	VG	CGMY
	$\sigma = 0.1361$	$\sigma = 0.1301$	$C = 0.6817$
		$\theta = -0.3150$	$G = 18.0293$
		$\nu = 0.1753$	$M = 57.6250$
			$Y = 0.8000$

Note that σ is the volatility of the diffusion term, while θ and ν represent the intensity and frequency of jumps, respectively, for the VG process. For the CGMY model, C determines kurtosis, G and M control skewness, and Y characterises the Lévy density. For further interpretation of the parameters, interested readers should refer to Carr et al. (2002).

Where numerical comparisons are performed with results presented in Luo and Shevchenko (2014), the parameter assumptions are different, such that they match those used in the paper. It will be made clear whenever parameter assumptions deviate from those in Table 1. All percentage rates used throughout this analysis are assumed to be per annum.

There are four parameters relating specifically to our algorithm:

- J , the number of discretisations of the investment account, W ;
- H , the number of discretisations of the guarantee account, A ;
- N , the number of Fourier-cosine series terms; and
- L , which determines the size of the truncation range $[a, b]$.

We conduct analysis of the convergence of the time zero value to 100 units by varying these parameters and observing the results.

4.1 Static Policyholder Withdrawal Behaviour

In this subsection we discuss the results of the COS framework as applied to static withdrawal behaviour. Firstly, an error analysis of Algorithm 1, presented in Appendix C, is explained along with a solution to the identified error. Having addressed the problem, we then compare numerical results of our framework to those presented in both Bacinello et al. (2014) and Luo and Shevchenko (2014) to demonstrate the consistency of the COS method with existing literature. We also analyse how quickly the COS method converges to the correct initial value. Finally, we investigate the sensitivity of the fair fee to various parameters.

4.1.1 Error Analysis

For numerical experiments, the infinite domain of the transition density function must be truncated to the interval $[a, b]$, as discussed in Subsection 2.3. This is achieved by selecting an appropriate L , for instance setting $L = 12$ covers practically the entire density function of any

return distribution. However, for accurate approximations, such a large coverage of the distribution is not necessary. For example, consider the standard normal distribution, where ± 5 standard deviations from 0 covers 99.9999% of the density, which coincides with the case where $L = 5$.

For the GMWB pricing problem, the motivation for reducing L stems from the fact that to compute the U_k coefficients, as in Equation (2.17), the full (discretised) range of values at the next time-step corresponding to $W_{t_m^-} \cdot e^y$, with $y \in [a, b]$, is required. The larger b is, the higher the necessary value of W_{\max} . This means that, for the same level of mesh fineness, we would require a higher number of discretisations of the investment account, J , which in turn increases the number of computations.

The results in Table 2 show that setting $L = 5$ does not provide accurate results for either the GBM or the VG distributions. Increasing the L parameter to 12 provides values closer to 100. However, this is at the expense of increasing the discretization points J of the investment accounts which increases the computational time.

Since the results in Table 2 do not quite converge to 100, even for $L = 12$, this prompted further investigation. In order to detect inaccuracies, we plot the contract values at different time-steps against the investment account values considered in Figure 3. Due to the guarantee component, we expect to see something resembling the value profile of a long call option. In this case, for low W the value should be reasonably flat, whereas when the guarantee is out-of-the-money the value should increase reasonably linearly with W .

As revealed in Figure 3, the expected shape of the curve is found in the final time-step (green). This is due to analytical expressions being available for U_k at maturity. Just one time-step back (red), there is an immediately noticeable error where the value drops off for high investment account values, for both $L = 5$ and $L = 12$. A similar error is identified in Ruijter et al. (2013), where the authors note that the error propagates recursively, resulting in an even more noticeable error at the first time-step (blue).

Although the error seems dramatic in both cases, by looking at the scale of the two x -axes one can determine why the $L = 12$ case is far more accurate. When L is high, the error does not occur at easily obtainable investment account values. For example, when $L = 12$, the blue line in Figure 3, corresponding to the first withdrawal date, only drops off substantially after the investment account is over 200. It is highly unlikely that the investment account doubles in value before the first withdrawal occurs, unless there are unrealistic parameters. On the other hand, for low L , the results in Table 2 demonstrate that the lower time zero value stems from the high probability of reaching the part of the time t_1 value curve in which there is undervaluation occurring.

The cause of the error is related to the earlier discussion regarding W_{\max} . For high values of W , it is not possible to consider the full range of returns, $y \in [a, b]$. In Figure 4, $W_{t_m^-}^{(1)}$ is an example

Table 2: Error analysis of Algorithm 1 for GBM and VG asset dynamics with $L = 5$ and $L = 12$.

(a) L=5				(b) L=12			
GBM		VG		GBM		VG	
J	V_0	J	V_0	J	V_0	J	V_0
20	103.66	20	74.39	20	220.79	20	770.23
80	91.53	80	92.60	80	99.23	80	104.51
400	91.82	400	92.97	400	99.37	400	101.55
1600	91.86	1600	93.03	1600	99.36	1600	100.56
3200	91.86	3200	93.03	3200	99.35	3200	100.38

Figure 3: Algorithm 1 error analysis at three points in time for different values of L .

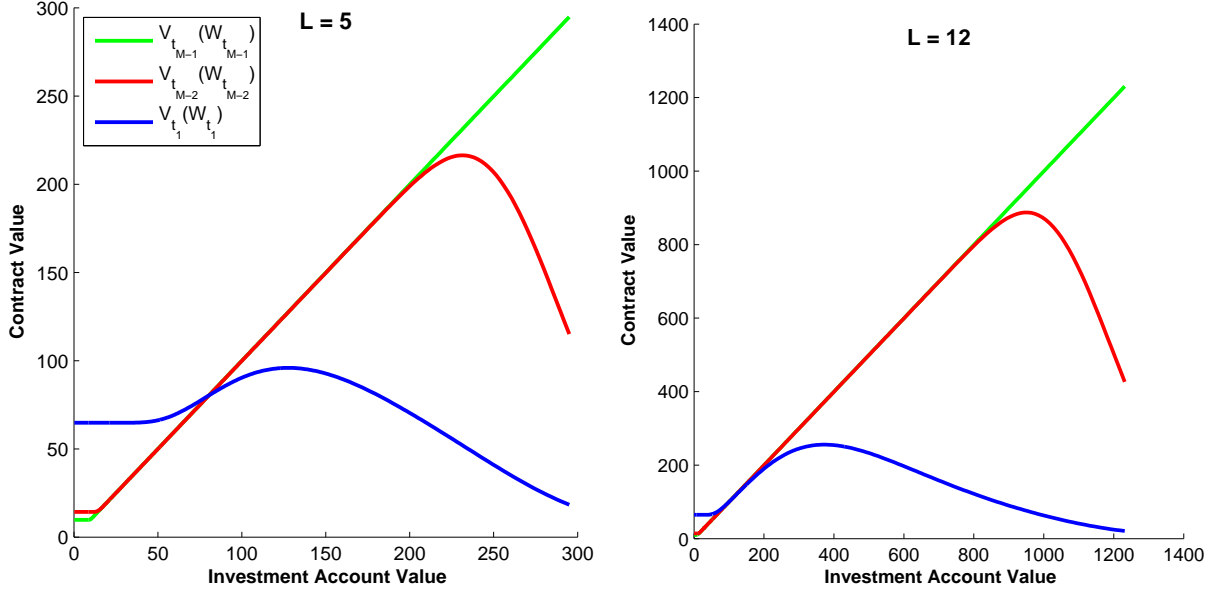
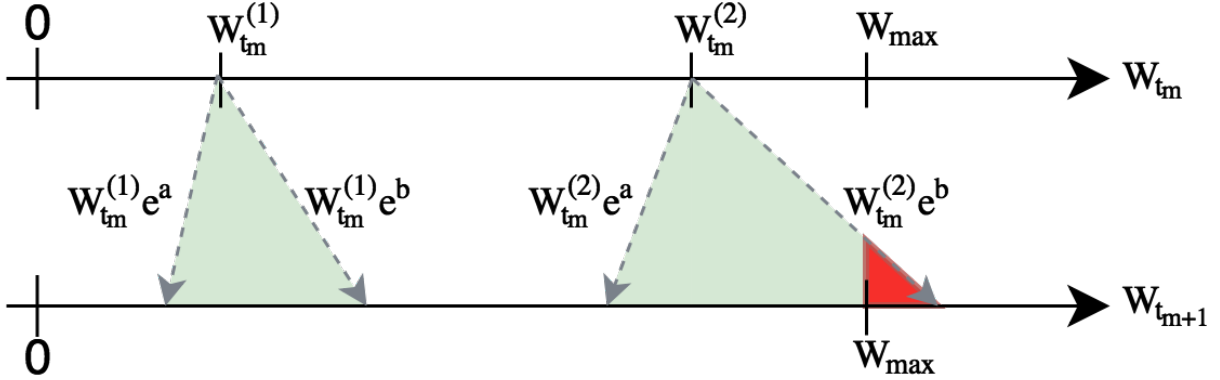


Figure 4: Illustration of the one-period asset return truncation range causing the investment account value to exceed W_{\max} .



of a W value where the full truncation range of one-period returns can be considered. On the other hand, $W_{t_m}^{(2)}$ demonstrates a point where a large return takes the investment account past W_{\max} at the next time-step, highlighted by the red region. Since the contract values are unknown for these higher points, aside from at maturity, the U_k coefficients for $W_{t_m}^{(2)}$ are not calculated over the whole truncation range, and thus cause the contract to become sharply undervalued.

Ruijter et al. (2013) suggest using extrapolation to avoid this error. To allow for lower values of L , this error is mitigated by employing simple linear extrapolation techniques to calculate the contract value at higher values of W . This method is suitable, due to the contract value being linear with respect to the investment account value when it is far out-of-the-money. This is confirmed by the linearity of the green lines in Figure 3, where the U_k terms have been calculated analytically. To confirm that this extrapolation provides accurate results, we value the contract using the same parameters as in Table 2 for the GBM case, but with the above-

mentioned change to the algorithm. As expected, we no longer see a bias below 100 for any of the L values in Table 3. Furthermore, the lower values of L converge for lower J , which aligns with the motivation for reducing L . Due to faster rate of convergence in J , we elect to use $L = 5$ for the numerical analysis.

Table 3: Convergence of V_0 to 100 for varying J and L with GBM asset dynamics – with extrapolation incorporated into Algorithm 1.

$J \backslash L$	5	8	12
20	101.48	330.22	3343.90
200	100.00	99.88	105.94
2000	100.00	100.00	99.57

4.1.2 Comparison of Results

We first perform numerical comparisons of our approach with that presented in Bacinello et al. (2014). We implement Algorithm 1, inclusive of the extrapolation technique discuss in the previous subsection. Furthermore, we implement discretely charged insurance fees to match the Bacinello et al. (2014) framework.

Table 4 demonstrates that the COS valuation framework yields fair fees consistent with those reported in Bacinello et al. (2014) across a variety of interest rates. The largest discrepancies, highlighted in pink, are differences of approximately 0.6 and 1 basis points (b.p.s). Clearly this is more of a concern in the CGMY case when $r = 0.07$, as the 0.6 b.p. represents a 20% difference. That said, it should be noted that Bacinello et al. (2014) reported results that are rounded to the nearest basis point, and a more precise comparison is not possible.

We further confirm the accuracy, and flexibility, of the COS method by comparing the results to those reported by Luo and Shevchenko (2014). Luo and Shevchenko (2014) report values obtained from finite difference (FD) techniques that had been used to price GMWBs in the early literature, such as Chen and Forsyth (2008), as well as their own approach using Gauss-Hermite quadrature aided by cubic splines (GHQC). Table 5 demonstrates the consistency of the COS method with existing literature across various maturities of the contract. The fair fees reported are for quarterly withdrawals with GBM asset dynamics with $r = 5\%$ and $\sigma = 20\%$. At each of the times to maturity considered, the three methods return the same fair fee accurate to at least one basis point.

Table 4: Comparison to Bacinello et al. (2014) fair fees for twenty-year GMWB contracts with varying risk-free interest rate, r .

Model $\backslash r$	3%	4%	5%	6%	7%
GBM	31.02 (31)	15.27 (15)	7.34 (7)	3.40 (3)	1.51 (1)
VG	64.02 (63)	38.27 (38)	23.10 (23)	13.94 (14)	8.36 (8)
CGMY	44.02 (43)	23.96 (24)	13.00 (13)	6.94 (7)	3.63 (3)

Table 5: Comparison to Luo and Shevchenko (2014) fair fees for GMWB contracts with GBM asset dynamics, $r = 5\%$, $\sigma = 20\%$, quarterly withdrawals and varying t_M .

Method \ t_M	10	12.5	20	25
COS	95.87	67.05	28.23	17.49
GHQC	95.81	66.99	28.33	17.59
FD	95.78	66.93	28.30	17.79

4.1.3 Computational Efficiency

Having confirmed that the results are consistent with existing valuation frameworks, we now look at the computational efficiency of the COS method framework.

Fang and Oosterlee (2008, 2009) demonstrate the rapid convergence of the COS method when evaluating European and Bermudan type options by increasing the N parameter, representing the number of terms in the Fourier-cosine series. The results in Table 6 confirm that this is still the case for GMWB valuation. As N increases from left to right across the rows in the GBM case, we observe no change in the approximated value. This indicates that convergence has already occurred at $N = 16$. For the VG case we expect to require a larger N parameter because the VG distribution is ‘less continuous’ (Fang and Oosterlee, 2008). This is observed in Table 6, where the number of COS summations required for convergence increases to $N = 64$ in the VG case.

Sufficient accuracy is obtained with the COS method for the GBM (resp. VG) when $J = 250$ and $N = 16$ (resp. $N = 64$), as noted in Table 6. The computational times highlighted in pink demonstrate the favourable performance of the COS method relative to the Bacinello et al. (2014) framework. The algorithm presented in Bacinello et al. (2014) uses FFT-based numerical techniques to approximate the probability density function and the recursion involves numerical integration of the recursive valuation integral. For the Bacinello et al. (2014) results, N refers to the number of discrete W points considered. The authors’ algorithm requires interpolation between mesh nodes, and increasing N is the only way to improve accuracy.

The keen observer will notice that, particularly for higher J , the computational time in the VG case is higher than the GBM case for the COS method (see green cells in Table 6), but relatively stable in the Bacinello et al. (2014) algorithm. This is caused by the skewness of the VG distribution, which leads to a larger truncation range, $[a, b]$, than in the GBM case. The increased computational time results from the need to approximate each U_k coefficient using a larger number of points.

4.1.4 Sensitivity Analysis

Existing literature provides a reasonably comprehensive analysis of the sensitivity of the GMWB fee to various parameters and underlying asset return distributions (Chen et al., 2008; Bacinello et al., 2014). In this subsection we confirm that the COS method produces consistent results with regards to the calculated fair fees in the static policyholder withdrawal behaviour case.

Similar to the valuation of financial derivatives, we expect to find that shifts in a parameter that increases the likelihood of the GMWB ending up in-the-money will increase the value of the contract. Therefore, the fair fee would have to rise, such that the time zero value of the GMWB remains at 100 units.

A further consideration is that, unlike financial derivatives, the insurer collects fees periodically to fund the GMWB. Additionally, the guaranteed rate, G , is higher for shorter-term maturities.

Table 6: Comparison of computational efficiency and accuracy between the COS method and Bacinello et al. (2014) framework, denoted Bac., with computational time in brackets reported in seconds.

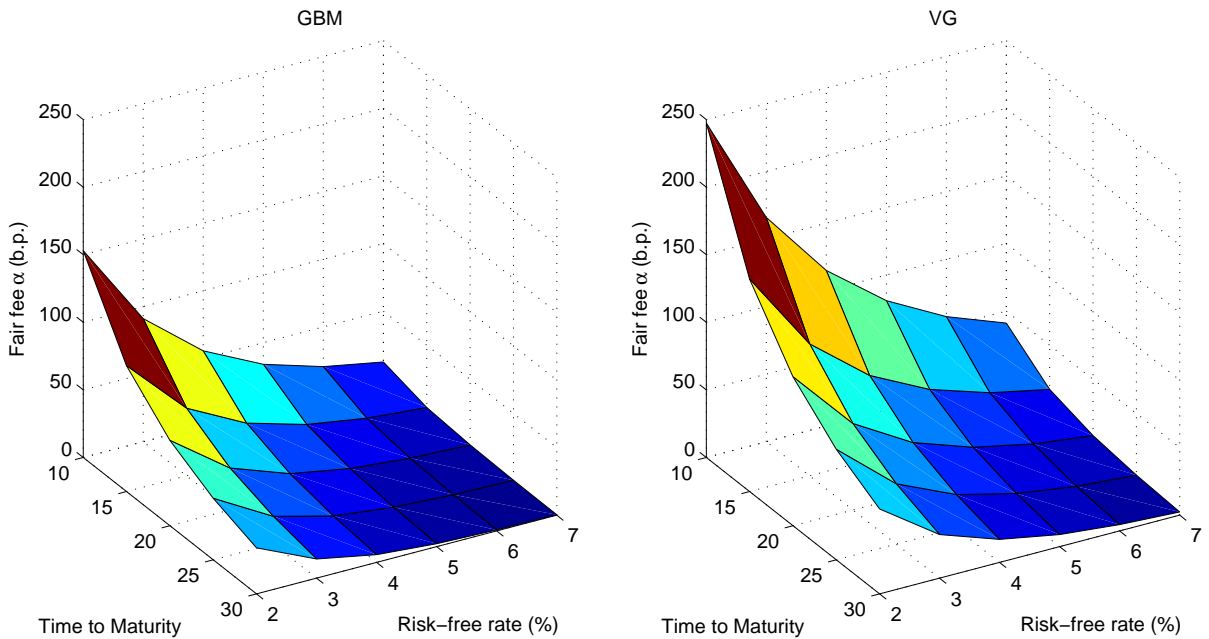
(a) GBM					(b) VG				
$J \backslash N$	16	32	64	128	$J \backslash N$	16	32	64	128
25	125.38 (0.014)	125.38 (0.015)	125.38 (0.016)	125.38 (0.019)	25	83.35 (0.013)	62.01 (0.014)	61.88 (0.017)	61.88 (0.020)
50	99.92 (0.027)	99.92 (0.029)	99.92 (0.035)	99.92 (0.044)	50	99.51 (0.027)	99.88 (0.032)	99.28 (0.039)	99.28 (0.053)
250	100.00 (0.181)	100.00 (0.294)	100.00 (0.317)	100.00 (0.449)	250	100.05 (0.204)	100.02 (0.285)	100.01 (0.444)	100.01 (0.815)
1000	100.00 (1.560)	100.00 (1.951)	100.00 (3.762)	100.00 (5.768)	1000	100.04 (1.965)	100.01 (4.716)	100.01 (6.242)	100.01 (9.408)
Bac.	110.73 (0.491)	102.3 (1.023)	100.49 (2.057)	100.06 (4.030)	Bac.	110.51 (0.496)	102.39 (1.002)	100.5 (1.977)	100.07 (3.960)

The combination of these two factors means that we expect to see higher fair fees for shorter-term contracts.

The surface plots in Figure 5 demonstrate that for both the GBM and VG cases, a shorter time to maturity results in higher fees. It is also apparent that the fair fees increase when the risk-free interest rate decreases. This is expected, because the lower risk-free interest rates make it more likely for the GMWB to become in-the-money. Finally, the fair fees in the VG case are higher than the GBM case. This is consistent with existing literature (Bacinello et al., 2014).

In Table 7 there is a very clear relationship between increasing the volatility of the stock return

Figure 5: Comparison of fair fees for varying time to maturity, t_M , and risk-free rate, r , with annual withdrawals and for both GBM and VG asset dynamics.



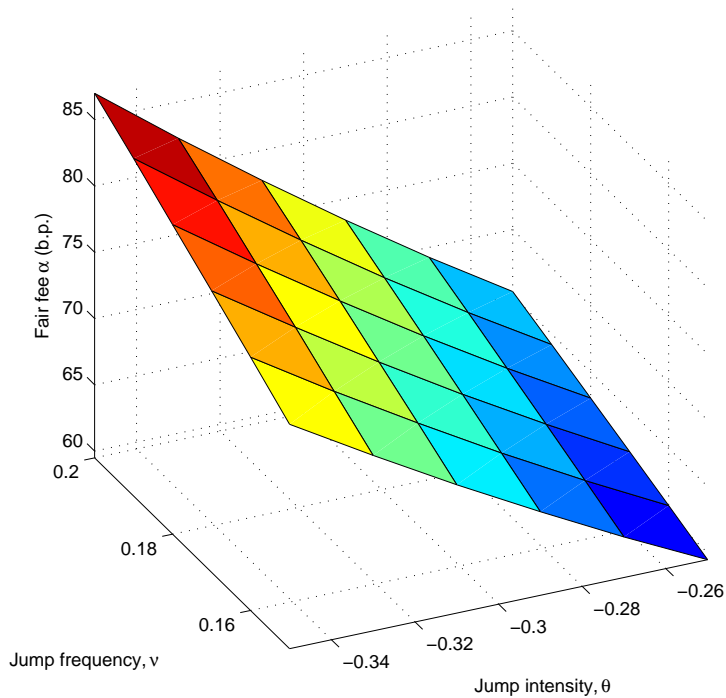
and an increase in the fair fee. For each of the times to maturity the fair fee increases by roughly three times from $\sigma = 0.15$ to $\sigma = 0.25$, which agrees with existing literature (Chen et al., 2008). For the VG case, it is apparent in Figure 6 that increasing the frequency, ν , and/or decreasing

Table 7: GMWB fair fees with GBM asset dynamics and varying σ and t_M .

$\sigma \backslash t_M$	10	15	20	25	30
15%	112.83	63.39	40.01	26.93	18.9
20%	199.06	117.02	76.82	53.59	38.84
25%	292.18	175.39	117.16	83.07	61.07

the intensity, θ , of jumps causes the fair fee to rise. Note that here, the decrease in jump intensity refers to the absolute value of the negative jumps becoming larger. This is consistent with the expectation that parameter changes that increase the likelihood of the GMWB being in-the-money increase the contract's value. In this example the GMWB has twenty annual withdrawals with $r = 5\%$ and $\sigma = 15\%$. We would expect these results to hold with other sets of these parameters.

Figure 6: Fair fees for a twenty-year GMWB with annual withdrawals, $r = 5\%$, $\sigma = 15\%$ and varying VG jump intensity and frequency parameters.



4.2 Dynamic Policyholder Withdrawal Behaviour

In this subsection we extend the analysis to the case of dynamic policyholder withdrawal behaviour. Again, the results confirm the consistency of the COS method with Luo and Shevchenko (2014).

4.2.1 Comparison of Results

The results in Table 8 confirm the consistency of the COS method under the dynamic policyholder withdrawal behaviour. Fair fees are found using the Luo and Shevchenko (2014) parameters of quarterly withdrawals, $r = 5\%$, and $\sigma = 20\%$. The largest discrepancy between the COS method and the other two approaches, highlighted in pink, is small relative to the fair fee being charged.

Table 8: Comparison to Luo and Shevchenko (2014) reported fair fees with GBM asset dynamics, varying t_M , two different penalty rates and quarterly withdrawals.

t_M	$\kappa = 5\%$			$\kappa = 10\%$		
	COS	GHQC	FD	COS	GHQC	FD
10	216.71	216.90	216.7	135.77	136.00	135.9
12.5	181.88	182.10	181.8	109.99	110.30	110.2
20	123.33	123.60	123.2	69.52	70.06	69.96
25	101.71	102.00	101.3	55.30	56.09	55.94

4.2.2 Convergence Properties

In Table 9 we look at the convergence of the COS method with respect to the J and H parameters. In this case, we substitute the fair fee, as presented in Luo and Shevchenko (2014) for a ten-year contract with quarterly withdrawals and a penalty rate of 10%, and observe the convergence of the initial contract value to 100. In Algorithm 2 of Appendix C, the set of possible withdrawal amounts is discretised at intervals of the same size as intervals between the discretised A account values. With the current parameters, the guaranteed rate is $G = 2.50$ at each withdrawal date.

We notice from Table 9 that when the number of discretisations of the guarantee account, H , is equal to 41, that is, the spacing between guarantee account values equals 2.50, the COS method converges to the correct value. However, we do not observe convergence for $H = 21$, where the difference between two account values is 5. This is because it is essential to consider the possibility of withdrawing exactly G at each time-step, which is the maximum allowed withdrawal to which no penalty applies. Also, for $H = 81$ and $H = 161$, since the spacings are exactly half and exactly a quarter of G , respectively, G is again considered as a withdrawal amount and we obtain highly accurate results. The convergence in J is similar to that observed in Table 6 for the static case. In this case, aside from when $H = 21$, we have two decimal point accuracy at $J = 250$.

Table 9: Convergence in J and H using the Luo and Shevchenko (2014) fair fee for a ten year contract with quarterly withdrawals, GBM asset dynamics, $r = 5\%$, $\sigma = 20\%$ and $\kappa = 10\%$.

$J \backslash H$	21	41	81	161
50	99.74	101.36	101.47	101.50
250	98.66	100.00	100.00	100.00
500	98.67	100.00	100.00	100.00

Due to being unable to replicate the results of Bacinello et al. (2014) in the dynamic case, and the fact that the method presented in Luo and Shevchenko (2014) is only capable of evaluating

the GMWB in the GBM framework, the convergence analysis of N here is performed differently to the static case. Having confirmed that our results are reliable in the previous subsection, we instead find the fair fee using the COS method itself, using large accuracy parameters, and substitute this fair fee to observe how quickly convergence occurs.

The results in Table 10 correspond to a fair fee that is found using $J = 1000$ and $N = 1024$ for a ten-year GMWB contract with annual withdrawals, and $r = \kappa = 5\%$. Keeping in mind the results of Table 6, where a similar analysis is performed in the static case, it is unsurprising that the GBM case experiences such fast convergence with increasing N . It is notable here that, under the CGMY asset dynamics, convergence occurs at $N = 32$, since the CGMY process generally experiences relatively slow convergence (Fang and Oosterlee, 2008).

Table 10: Convergence in the dynamic case for a GMWB contract with ten annual withdrawals using a fair fee calculated with $J = 1000$ and $N = 1024$, with $r = \kappa = 5\%$ and varying J and N .

(a) GBM					(b) CGMY				
$J \backslash N$	16	32	64	128	$J \backslash N$	16	32	64	128
25	128.20	127.86	127.85	127.85	25	109.06	118.99	118.99	118.99
50	100.06	100.07	100.07	100.07	50	100.06	99.96	99.96	99.96
250	100.02	100.00	100.00	100.00	250	100.26	100.00	100.00	100.00
500	100.01	100.00	100.00	100.00	500	100.08	100.00	100.00	100.00

4.2.3 Sensitivity Analysis

Similar to the static case, the option-like features of GMWB contracts mean that we expect their value to increase as the likelihood of being in-the-money increases.

As expected, the results in Figure 7 show that at varying times to maturity, the fair fee increases as r decreases, under both the GBM and VG dynamics. Furthermore, like in the static case, shorter times to maturity require higher fair fees.

The purpose of the penalty fee imposed on withdrawals over the guaranteed amount is primarily to discourage early surrender of the GMWB. Figure 8 illustrates that higher penalty fees cause lower fair fees, thus indicating a reduction in the GMWB's value. Judging by the relative flatness of the surfaces for $\kappa \geq 6\%$, it appears that setting the penalty to 6% is enough to discourage most of the cases where a policyholder may otherwise have chosen to withdraw above the guaranteed rate, G .

The reset provision applies a further penalty to the policyholder. Therefore, we expect it to reduce the value of the fair fee, as is shown in Table 11. However, the effect is low in relative terms, which suggests that there are few circumstances where the optimal withdrawal strategy would involve withdrawing $\gamma_{t_m^-} > G$ that corresponds to when $W_{t_m^-} < A_{t_m^-}$. In other words, it is unlikely for the reset provision to actually cause the guarantee account to drop by more than the withdrawal amount. This observation is consistent with the results presented in Chen et al. (2008).

4.3 Hedging Results

In this subsection we compare various hedging strategies. First we test and confirm the accuracy of the COS method for calculating the Greeks of a European put option, as well as the moments

Figure 7: Comparison of fair fees for annual withdrawals with $\kappa = 5\%$ and varying risk-free rate, r , and time to maturity, t_M , with dynamic withdrawals.

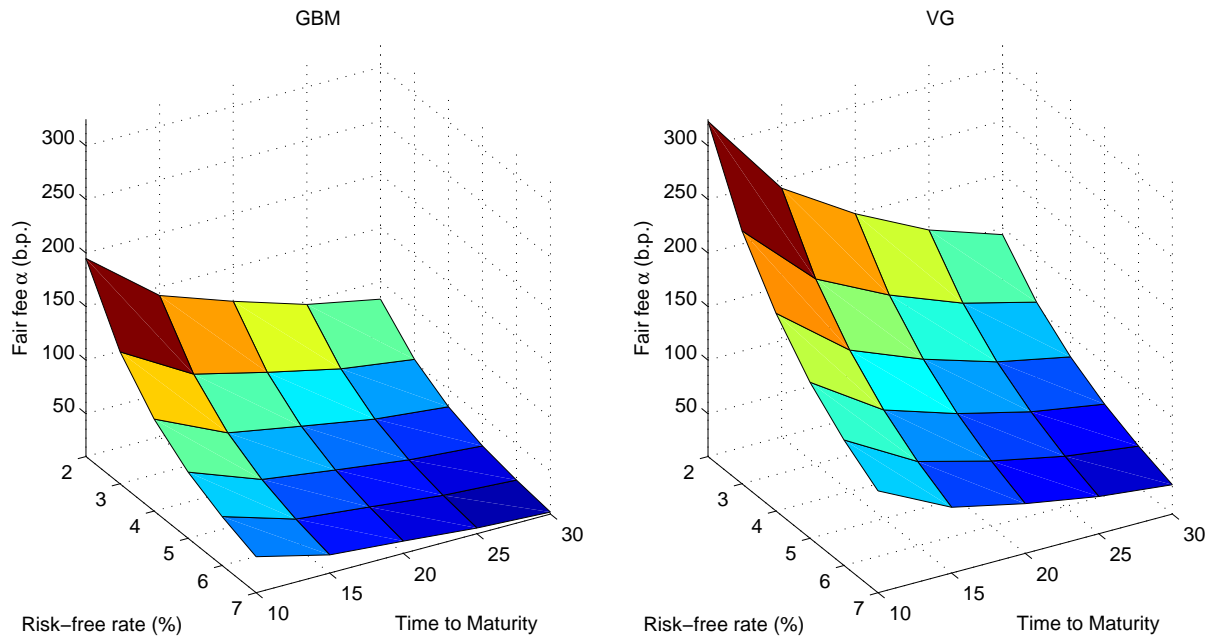


Figure 8: Comparison of fair fees for a GMWB contract with twenty annual withdrawals and varying risk-free rate, r , and penalty fee, κ .

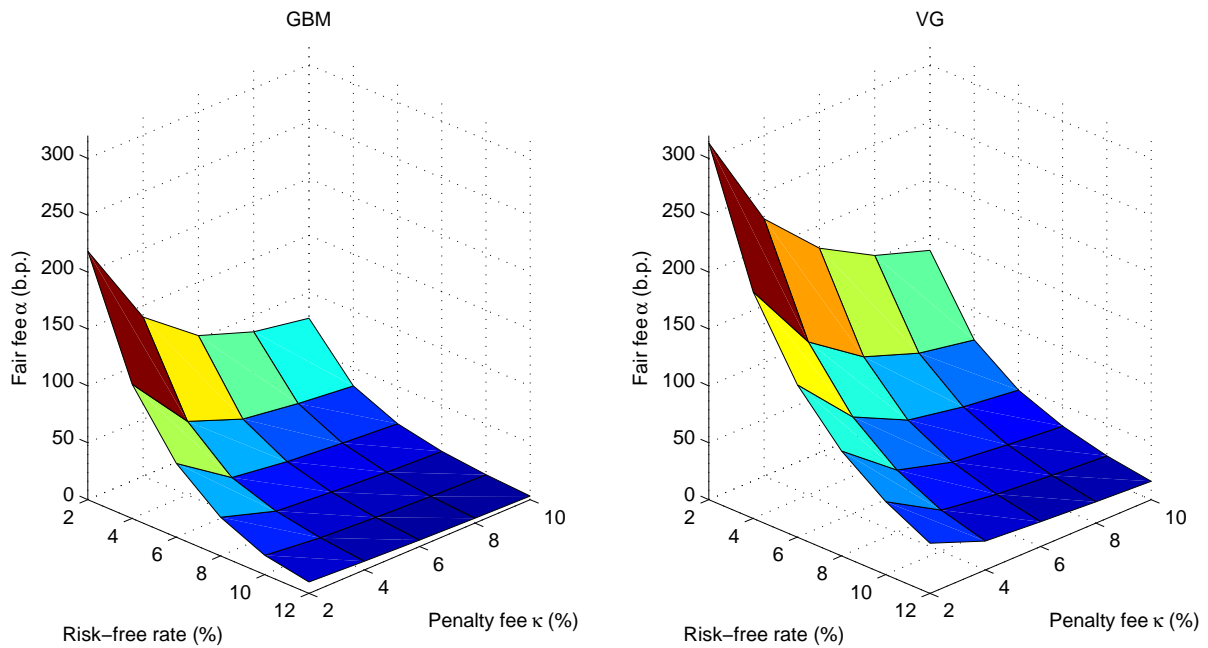


Table 11: Effect of the reset provision on the fair fees of a ten-year GMWB with quarterly withdrawals, $r = \kappa = 5\%$ and varying σ .

σ	15%	20%	25%	30%
No reset	103.67	216.86	344.93	470.86
Reset	97.46	201.37	330.67	457.08

and quantiles of a portfolio distribution. We then investigate six examples of hedging under different circumstances with various hedging strategies.

4.3.1 COS Method Approximations

The European option pricing approximation, given by Equation (3.3.1), has been proven to display rapid convergence to the actual option prices (Fang and Oosterlee, 2008). However, a numerical analysis of the Greeks formulae, Equations (3.3.1) and (3.3.1), is not provided in Fang and Oosterlee (2008), where the equations are derived.

Table 12 contains COS method approximations and analytic solutions for the delta and gamma of a European put option on a stock with an initial price of 100, time to maturity of one year, a risk-free interest rate of 5% and volatility of 20% in the Black-Scholes framework. These values are calculated for different strike prices, K . It is evident that the COS method converges rapidly to the analytic solutions for in-the-money, at-the-money and out-of-the-money options.

To check the accuracy of the COS method in determining moments of the hedging loss distribution, we give an example of a portfolio that starts with one unit of value and accumulates over a year according to GBM asset dynamics with $\mu = 10\%$ and $\sigma = 20\%$ using real-world probabilities. In Table 13 we see that, for both the second and third moments, convergence occurs rapidly, with at least three decimal point accuracy at $N = 32$.

Table 12: COS approximation of the delta and gamma for in-, at- and out-of-the-money European puts compared to the analytic solutions.

		N				Analytic
		8	16	32	512	
Δ	75	-0.0681	-0.0357	-0.0369	-0.0369	-0.0369
	100	-0.3668	-0.3636	-0.3632	-0.3632	-0.3632
	125	-0.7027	-0.7772	-0.7781	-0.7781	-0.7781
Γ	75	0.0069	0.0041	0.0040	0.0040	0.0040
	100	0.0140	0.0185	0.0188	0.0188	0.0188
	125	0.0150	0.0152	0.0149	0.0149	0.0149

Table 13: COS approximation of statistical moments of a portfolio following GBM asset dynamics over one year with $\mu = 10\%$ and $\sigma = 20\%$ under real-world probabilities.

Moment		N				Analytic
		16	32	64	128	
Second		1.259	1.271	1.271	1.271	1.271
Third		1.377	1.522	1.522	1.522	1.522

Lastly, we check the accuracy of using the COS method to calculate the quantile-based risk measures of the hedging loss distributions. Table 14 shows the results of approximating the VaR and TVaR of a portfolio starting with one unit, whose assets again follow GBM dynamics with mean return of 10% and a volatility of 20%. The number of terms in the Fourier-cosine series, N , used to calculate the densities can be set very high. Here, we use $N = 2^{14}$ to calculate the density values. Of more interest is the convergence with regards to J , the number of next period portfolio value discretisations. Table 14 reveals that a relatively high value of J is required to converge to the analytic VaR. For the VaR and TVaR measures, reasonable accuracy seems to occur by the time VaR has converged at $J = 2^{11}$.

When performing these quantile-based calculations, the primary computational expense comes from sorting the hedging loss distribution. The time required to sort a vector increases by a factor of $n \log n$ where n is the size of the vector. Thus, it is beneficial to use the COS method and sort a vector of size 2^{13} , which is roughly 1000 times smaller than the vector of size 10^7 used for the Monte Carlo simulations in Table 14.

Table 14: COS approximation of 95% VaR and 95% TVaR for a portfolio driven by real-world GBM asset dynamics with $\mu = 10\%$ and $\sigma = 20\%$ compared with the analytic solution for the 95% VaR and approximations found using Monte Carlo simulations (MC).

Measure \ J	2^7	2^9	2^{11}	2^{13}	Analytic	MC (10^7 sims.)
95% VaR	1.544	1.546	1.536	1.536	1.536	1.535
95% TVaR	1.602	1.684	1.672	1.671	-	1.674

4.3.2 Hedging Strategy Examples

This subsection demonstrates the flexibility of the hedging framework with several examples. As discussed in Subsection 3, the framework allows us to form hedging portfolios for delta and delta-gamma hedges, and more notably to construct local risk minimisation hedging strategies for a wide variety of risk measures. Since the risk measures are minimised under the real-world probabilities, the expected market return is assumed arbitrarily to be 12%.

Similar to the numerical analyses presented in Coleman et al. (2007) and Kolkiewicz and Liu (2012), we demonstrate that the local risk minimisation hedging strategies do not rely on having a large selection of options from which to choose. This is done by allowing for different combinations of in-, at- and out-of-the-money European puts and calls to be traded in each example.

First Example

Here we present an example similar to that of Kolkiewicz and Liu (2012), in order to demonstrate the robustness of risk minimisation hedging strategies compared with hedging the Greeks in the presence of asset dynamics with jumps or infrequent portfolio rebalancing dates. When delta and delta-gamma hedging the GMWB, the insurer tries to ensure that movements in their assets and liabilities, caused by shifts in the underlying asset's value offset each other. Thus, the hedging loss is the change in net liability (that is, the change in liabilities minus the change in assets). For inter-withdrawal date hedging we calculate this change in net liability as

$$\underbrace{\left(V_{t_{m+1}} \left(W_{t_{m+1}}^- \right) - V_{t_m} \left(W_{t_m}^- \right) \right)}_{\text{Liabilities}} - \underbrace{\left(W_{t_{m+1}}^- - W_{t_m}^- \right)}_{\text{Assets}},$$

such that the GMWB's value represents the insurer's liability, and the investment account value represents the insurer's assets. Note that we ignore other assets the insurer may be holding. We assume that short-selling of derivatives is limited to one unit of each of the available options. The available options comprise a variety of ten in-the-money, at-the-money and out-of-the-money European puts and calls.

Kolkiewicz and Liu (2012) find that the Greeks hedging strategies perform well in the GBM framework, particularly as the frequency of portfolio rebalancing increases. When jumps are introduced to the asset dynamics, through the Kou (2002) model, the Greeks hedging strategies break down, while the local risk minimising strategy remains robust.

Figures 9 to 15 which are presented throughout this section show the estimated, smoothed probability density functions for the hedging loss distributions. It should be noted again that a loss is *positive* and a gain is *negative* in these distributions. These are constructed using Equation (2.10), the COS method density approximation, to calculate the density of stock return realisations that correspond to each hedging loss. The density function is approximated using the techniques discussed in Subsubsection 3.2.2. This is done with hedging losses, inclusive of the cost of the hedging portfolio, that are known at discrete points.

Figure 9 demonstrates the effectiveness of hedging the Greeks compared with hedging the second moment of the hedging loss for both annual and quarterly withdrawal dates with GBM account dynamics. In the annual withdrawal case, the second moment hedge clearly outperforms the other hedges. We conclude this because the second moment hedge is much more centered around a zero hedging loss, which is ultimately the aim for hedging the second moment or the Greeks. This result is expected, as the theory behind hedging the Greeks relies on continuous (or very frequent) portfolio rebalancing. Since the rebalancing is only allowed at withdrawal dates, the Greeks hedging strategies are ineffective in the annual withdrawals case. However, in the quarterly withdrawals case we see a drastic improvement in the Greeks hedging strategies. The delta-gamma hedge appears to have a slightly shorter, and therefore more favourable, right tail than the second moment hedge and is almost as peaked. For these reasons we conclude that the delta-gamma hedge outperforms the second moment hedge in the quarterly withdrawal case.

A similar plot is shown in Figure 10, where the fund dynamics are instead driven by a VG process. In all cases the hedging loss distribution are noticeably less peaked. In the annual withdrawal case, the second moment hedge is the only effective hedge. While the Greeks hedges are still largely ineffective in the quarterly withdrawal case, they do begin to form peaks around zero. Since the Greeks hedges are less peaked and have fatter tails than the second moment hedge, they remain outperformed by the risk minimisation strategy.

The results in this example are consistent with those presented in Kolkiewicz and Liu (2012). In the remaining examples we will solely compare various risk measures for use in local risk minimisation hedging strategies.

Second Example

In this second example we compare the 95% VaR and first moment of the hedging loss as the risk measures to minimise. The insurer is again attempting to hedge the change in net liabilities. There are two European puts, one in- and one out-of-the-money, and one at-the-money European call available, no short selling is allowed, and the budget constraint is 0.5% of the investment account value.

Figure 11 displays both the observed hedging losses incurred for different realisations of $W_{t_{n+1}}$, in the top panel, and smoothed probability density functions for the hedging loss, in the bottom panel.

From Figure 11, it is clear that the hedges cut off the maximum hedging loss. This can be seen in the top panel, where, unlike the unhedged portfolio, the hedging loss of the hedged portfolios for any of the possible investment account values at the next withdrawal date, $W_{t_{m+1}}$, either flattens out, in the 95% VaR hedge, or reaches a peak, in the first moment hedge. There is no doubt that the 95% VaR hedge has a lower 95% VaR than either the unhedged, or first moment hedged portfolios. This is observed in the bottom panel of Figure 11, where the density of the 95% VaR hedged portfolio cuts off earlier than the other two portfolios.

In Table 15 it can also be concluded that the first moment is lowest for the first moment hedged portfolio. Although the probability density functions in figures throughout this analysis have been smoothed, the statistics presented in Table 15 and other similar tables in the remainder of this section are calculated using the raw density functions.

Figure 9: Hedging the Greeks under GBM dynamics with annual (top) and quarterly (bottom) withdrawals.

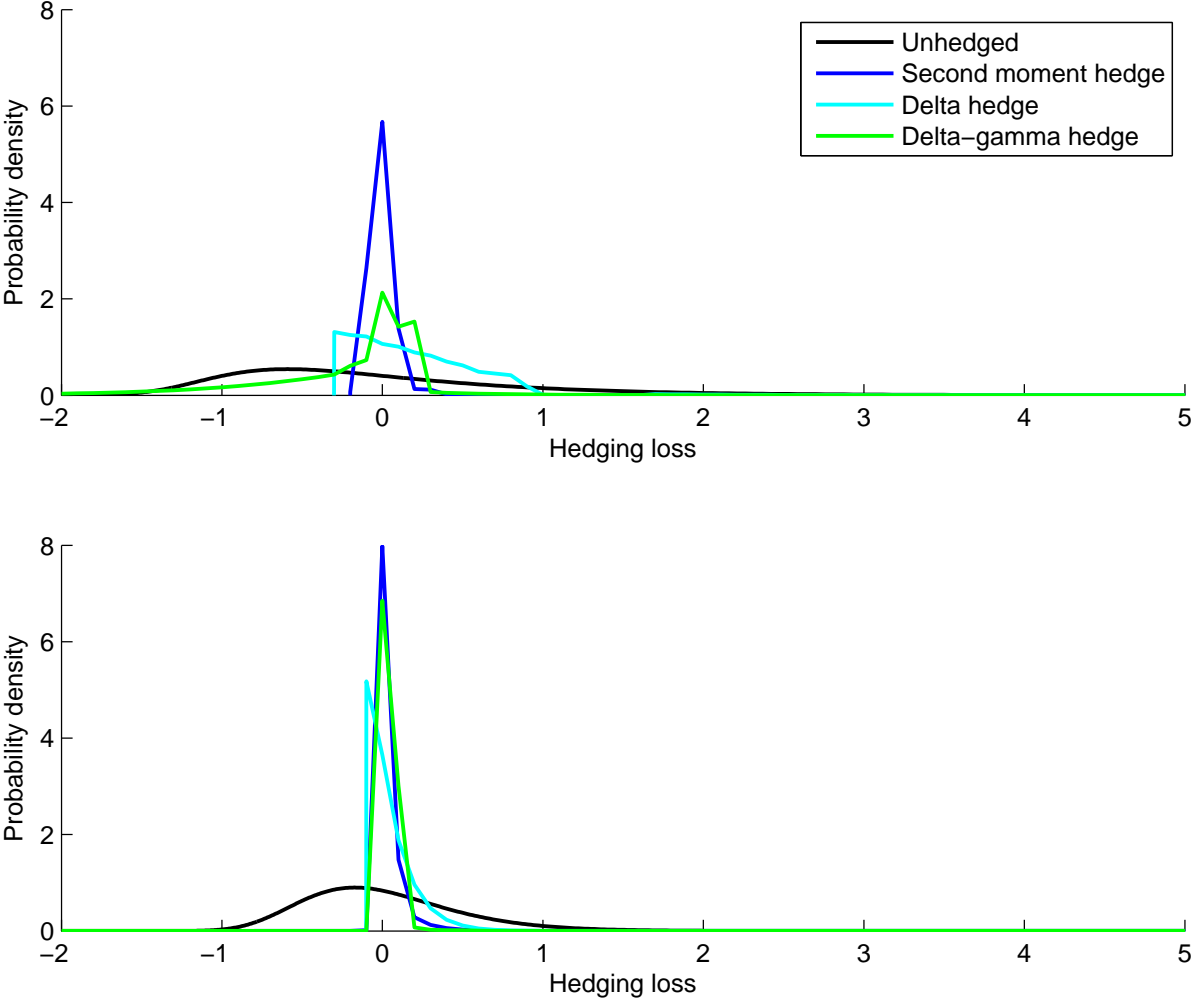


Figure 10: Hedging the Greeks under VG asset dynamics with annual (top) and quarterly (bottom) withdrawals.

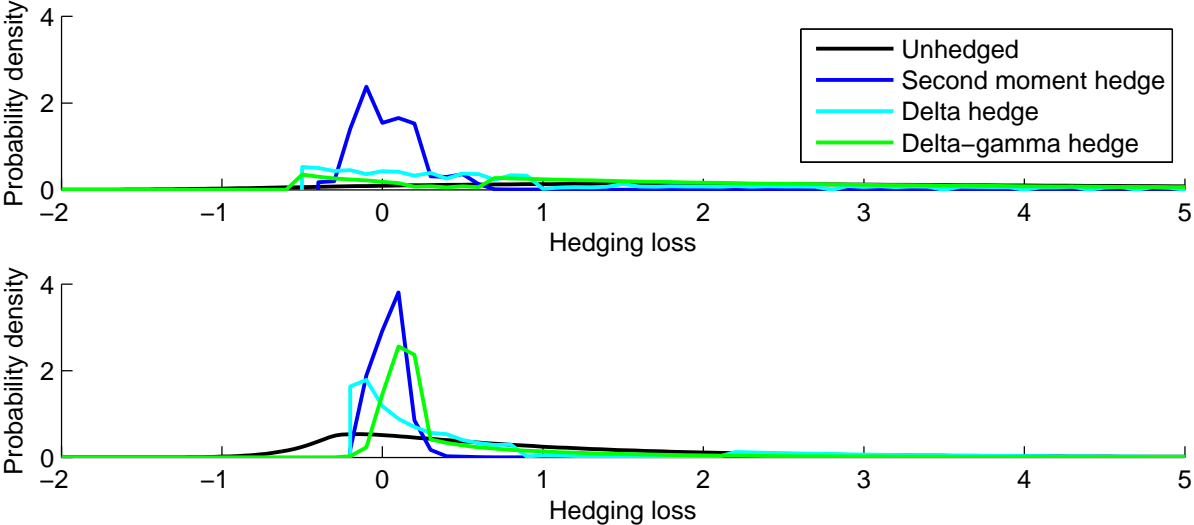
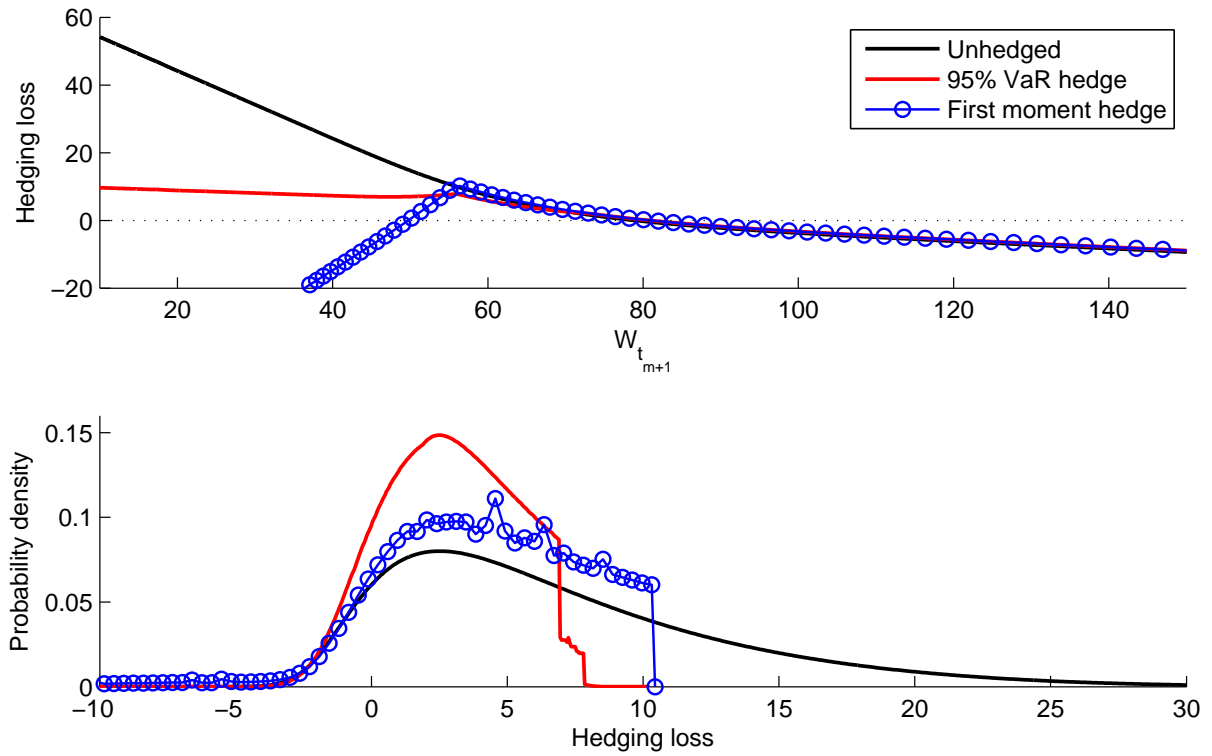


Figure 11: Example of hedging the 95% VaR and first moment of the hedging error with VG asset dynamics.



Interestingly, both these hedges reduce the first moment of the hedging loss simultaneously with the other statistics such as variance or 95% VaR. The use of hedging to reduce the potential losses of a portfolio often comes at the cost of reduced profitability. Here, the unhedged insurer faces a reasonably unfavourable hedging loss distribution. However, since the hedging loss is higher when the stock price, and therefore the investment account value, drops, the upper tail of its hedging loss can be cut short using cheap, out-of-the-money European puts. This relationship can be seen in the top panel of Figure 11.

Table 15: Statistics for Second Example – risk minimisation of the change in net liability with no short-selling.

Hedge	Cost	First mom.	Variance	95% VaR	99.5% VaR	90% TVaR
Unhedged	-	5.29	36.09	19.25	28.80	20.41
95% VaR	0.45	3.56	7.68	6.59	7.51	6.65
First moment	0.45	2.79	23.71	9.63	10.36	9.62
Second moment	0.45	3.32	7.22	8.14	8.51	8.10

The statistics for the second moment hedge have also been presented in Table 15. While Kolkiewicz and Liu (2012) choose to hedge the second moment of the hedging loss, these results highlight that the insurer could significantly reduce the 95% and 99.5% VaR of the change in net liability, albeit at the cost of a slightly higher expected loss and variance, by instead minimising the quantile-based risk measure. For an insurer, it may be preferred to take on the increase in expected loss and variance, if the lower VaR measures result in reduced capital requirements.

Third Example

Again for this example, the hedging performance of two risk minimising portfolios is compared when hedging the change in net liability. The risk measures considered are the 90% TVaR and the second moment. In this case, the budget is limited to a portion of the fee received at time t_m , but up to one unit of each of the options may be short sold. Similar to an example in Coleman et al. (2007), the assumed available options include just one in-the-money put option and one out-of-the-money call option.

Table 16 and Figure 12 reveal that, in this example, the two hedging portfolios end up being the same. It is more difficult to form a hedging portfolio when the available hedging instruments are so limited. However, we do see in Table 16 that the variance, VaR and TVaR metrics are all lower for the hedged portfolios, while the first moment of the hedging loss is also reduced. Therefore, we conclude that the hedged portfolios in this case still outperform the unhedged portfolio.

Figure 12: Example of hedging the 90% TVaR and second moment of the hedging error with VG asset dynamics.

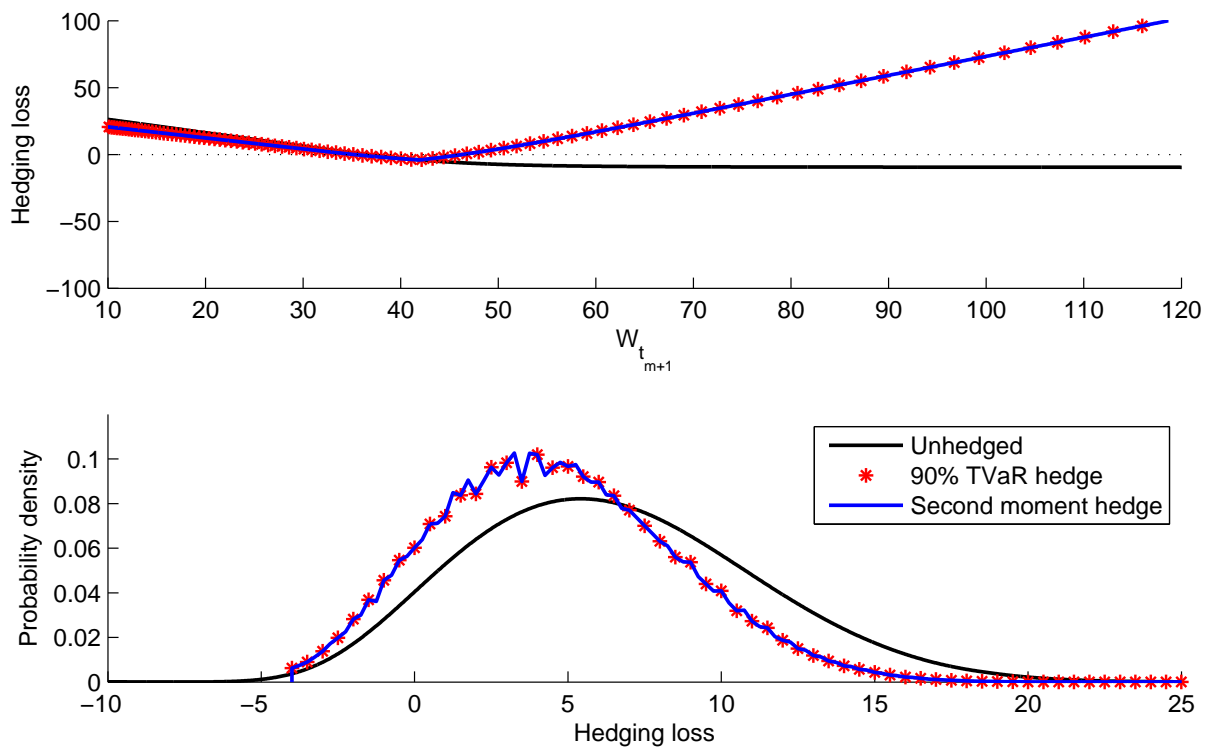


Table 16: Statistics for Third Example – risk minimisation of the change in net liability with short-selling allowed.

Hedge	Cost	First mom.	Variance	95% VaR	99.5% VaR	90% TVaR
Unhedged	-	7.04	25.08	14.69	19.47	15.26
90% TVaR	0.0039	4.85	16.90	11.45	15.33	11.87
Second moment	0.0039	4.85	16.90	11.45	15.33	11.87

Fourth Example

In the previous examples, we assume that the uncertainty to be hedged is the change in net liabilities. Instead, this example demonstrates the flexibility of the framework by hedging the

cash flow to be received by the insurer at the next time period, such that

$$H_{t_{m+1}} \left(S_{t_{m+1}} | W_{t_n^+}, S_{t_m^-} \right) = -\alpha(t_{m+1} - t_m) \cdot W_{t_{m+1}}, \quad (4.0)$$

where α is the discretely charged fee. The risk measures considered in this example are the 95% VaR and the variance of the hedging loss. The budget is constrained to 10% of the fee received at time t_m , with no short-selling allowed.

In this case, since $W_{t_{m+1}}$ is bounded below by zero, the unhedged loss is bounded above by zero. It should be noted once more that negative hedging losses are favourable.

As can be seen in Figure 13, both of the hedged portfolios have a very similar maximum loss and maintain a left tail, corresponding to receiving an increased fee. For these reasons, the hedged portfolios both outperform the unhedged portfolio.

Again, the insurer will have to decide whether it is more important to reduce the volatility of the loss or the VaR metrics. For this hedging uncertainty, it is less likely that the VaR metrics of the hedging loss will have an impact on any capital requirements, and thus may have less influence on the insurer's hedging decision. Table 17 reveals that the variance hedged portfolio has a slightly lower expected hedging loss, which could make this hedging strategy preferable.

Figure 13: Hedging the fee received at the next period under VG asset dynamics.

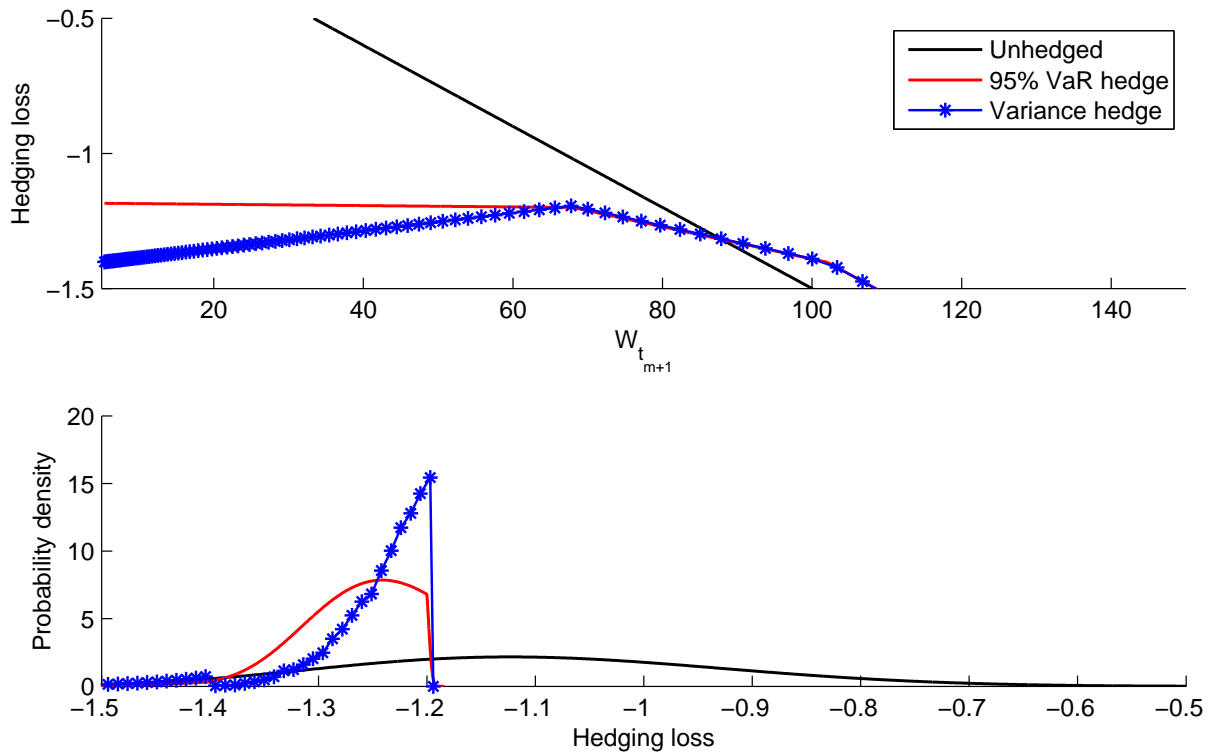


Table 17: Statistics for Fourth Example – risk minimisation of the fee received by the insurer at the next withdrawal date.

Hedge	Cost	First mom.	Variance	95% VaR	99.5% VaR	90% TVaR
Unhedged	-	-1.067	0.0340	-0.789	-0.614	-0.769
95% VaR	0.128	-1.239	0.0024	-1.205	-1.197	-1.204
Variance	0.128	-1.247	0.0019	-1.197	-1.194	-1.197

Fifth Example

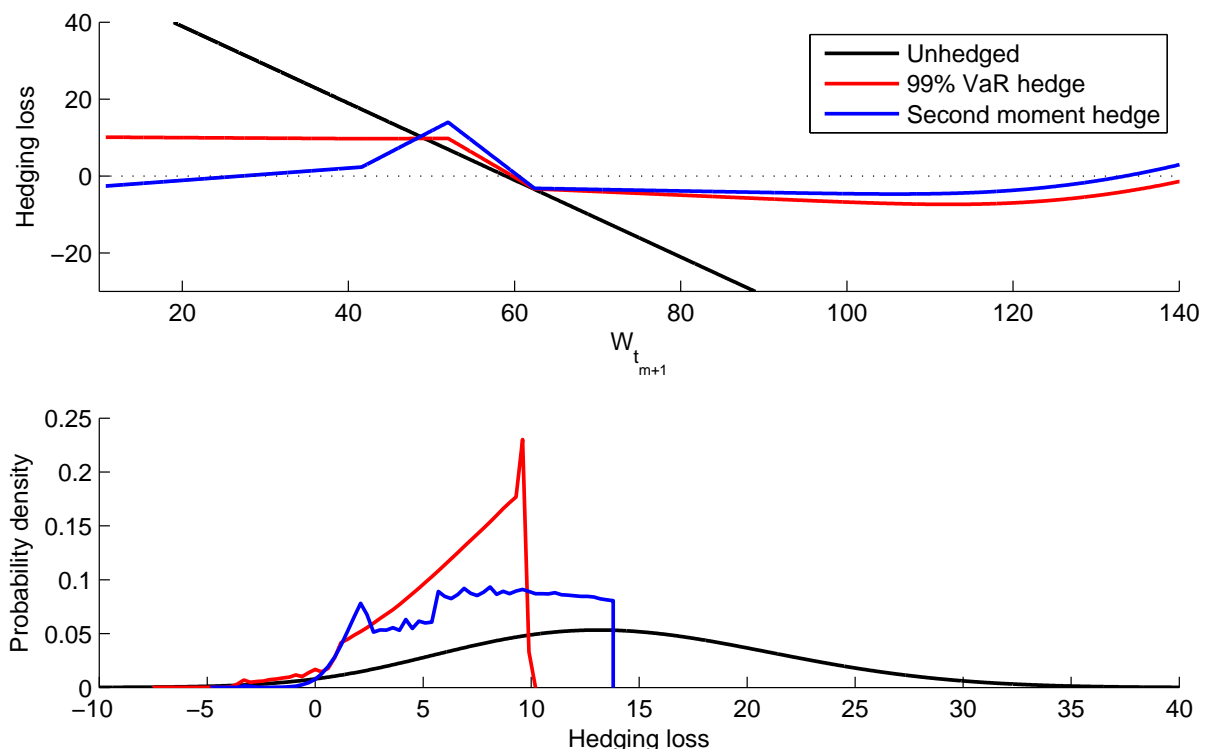
Here we consider, again, hedging the change in net liability. However, we instead assume dynamic policyholder behaviour, with VG asset dynamics. Due to the increased range of withdrawal amounts available to the policyholder, we expect to see greater variability in the hedging losses. This is because the policyholder's decision is essentially maximising the insurer's liability, and also because of the interactions between the penalties applied to withdrawals.

The performance of hedging the 99% VaR and second moment risk measures is compared. It is assumed that there is one out-of-the-money call, one in-the-money put and one out-of-the-money put available. The budget constraint is 0.5% of the investment account value, and short-selling is limited to one unit of each derivative.

The resulting hedging portfolios each seem to outperform the unhedged portfolio. In the top panel of Figure 14, it is clear that the hedged portfolios limit the maximum hedging loss, at the cost of a higher density at these lower hedging losses. We further note in Table 18 that the hedged portfolios have a lower first moment and variance than the unhedged portfolio.

In the bottom panel of Figure 14 we see that the lower tail of the loss distribution is highest for the 99% VaR hedge, indicating a higher probability of making a profit. However, coming back to Table 18, note that this portfolio has a higher first moment than the second moment hedge. Similar to the second example, an insurer may wish to sacrifice a lower first moment for reduced VaR metrics. In Figure 15 we compare the static and dynamic policyholder withdrawal

Figure 14: Example of hedging the 99% VaR and second moment of the hedging error under VG asset dynamics with dynamic policyholder withdrawal behaviour.



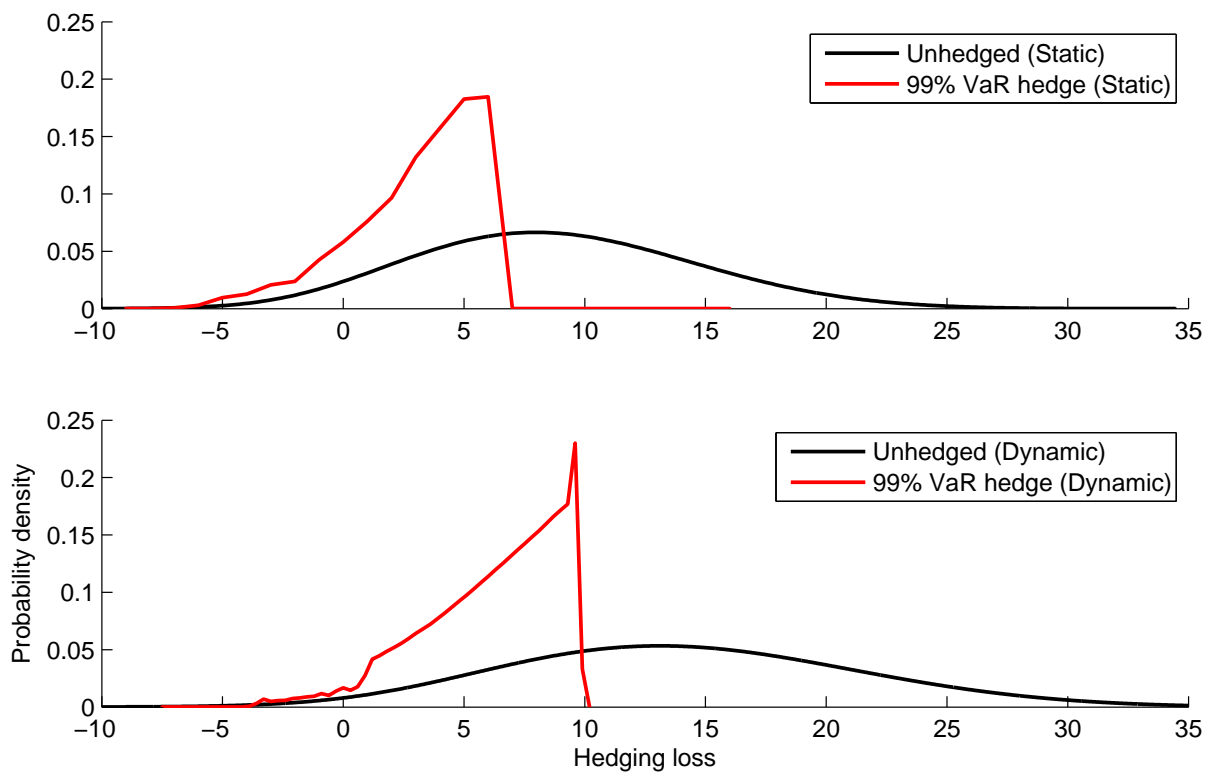
behaviour assumptions, using the exact same parameters. The static results, in the top panel, are notably shifted to the left. This is due to using the same insurance fee for both cases, when the fair fee would be lower for the static case. The unhedged curve has a noticeably lower spread in the static case. This is because of the restricted withdrawal decisions. For the hedged curves,

the spread achieved in each case is very similar, with the bulk of the density looking roughly the same, albeit with a shift. The risk minimisation hedging strategy is robust with different behavioural assumptions.

Table 18: Statistics for Fifth Example – risk minimisation of the change in net liability with dynamic policyholder withdrawal behaviour.

Hedge	Cost	First mom.	Variance	95% VaR	99.5% VaR	90% TVaR
Unhedged	-	15.429	57.924	26.714	33.882	27.546
95% VaR	0.136	9.204	3.405	9.576	9.793	9.559
Second moment	0.260	5.375	17.957	13.295	13.896	13.306

Figure 15: Comparison of hedging with static and dynamic policyholder withdrawal behaviours.



Sixth Example

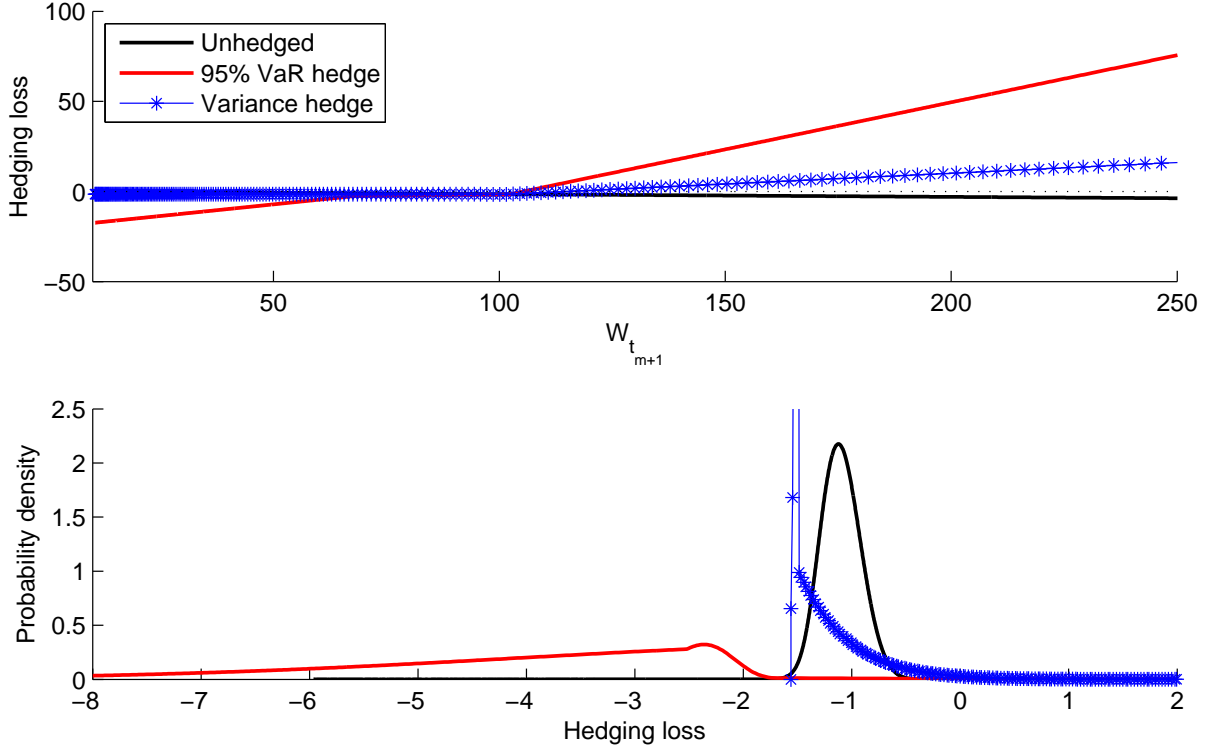
Similar to the fourth example, here we consider hedging the cash flow received by the insurer, given by Equation (4.3.2). In this example we consider the dynamic case under VG asset dynamics. The budget is constrained to half of the fee received at the current withdrawal date, and shorting is limited to one unit for each option. The options available are one out-of-the-money call, and one out-of-the-money, one in-the-money, and one at-the-money put.

For the dynamic case, there is a potential for the policyholder to surrender the contract, and thus no fee will be extracted from the investment account at the next time period. We choose an example where the policyholder does not surrender at the current withdrawal date, since there would then be nothing to hedge at the next time period.

The bottom panel in Figure 16 seems to demonstrate favourable hedging loss distributions for each of the hedged portfolios, compared with the unhedged curve. However, the top panel

reveals that the insurer becomes exposed to very large losses. This may be a concern regardless of how unlikely these losses are. Table 19 reveals that, although the 95% VaR is substantially

Figure 16: Hedging the fee received at the next period under VG asset dynamics with dynamic policyholder withdrawal behaviour.



lower for the 95% VaR hedged portfolio, the 99.5% VaR is also much larger. Furthermore, the 95% VaR hedged portfolio has a massive variance in comparison to the unhedged and variance hedged portfolios. While the first moment is also substantially lower than for the 95% VaR hedge, an insurer may not be willing to face such a large 99.5% VaR or variance.

Table 19: Statistics for Sixth Example – risk minimisation of the fee received by the insurer at the next withdrawal date with dynamic policyholder behaviour.

Hedge	Cost	First mom.	Variance	95% VaR	99.5% VaR	90% TVaR
Unhedged	-	-1.067	0.034	-0.789	-0.614	-0.769
95% VaR	-0.210	-3.297	3.103	-2.069	1.314	-1.542
Variance	-0.038	-1.523	0.001	-0.491	0.403	-0.377

5 Conclusion

This research provides a framework within which variable annuities embedded with GMWB riders can be priced and hedged using the COS method. By using the COS method, we are able to explore the effect of different Lévy processes on various aspects of the model. We find that convergence occurs rapidly for both the static and dynamic policyholder withdrawal behaviour assumptions, and for the GBM, VG and CGMY asset dynamics. We have been able to confirm that the computational speed of the COS method outperforms the FFT-based techniques used

in Bacinello et al. (2014) for the static case. The framework presented can easily incorporate complex contract features such as the reset provision without losing convergence speed and accuracy.

We further extend use of the COS method to assist in forming hedging strategies that seek to minimize a risk measure. Here we study both moment and quantile-based risk measures such as the variance of the hedging outcomes or the 95% VaR of the hedged portfolio loss distribution. The risk-minimization hedging strategies considered outperform the unhedged or delta-gamma hedge strategy, especially for infrequent portfolio rebalancing dates in line with the literature. The framework developed proves to be compatible to both pricing, delta-gamma hedging, risk minimization and VaR calculations, making it a strong candidate for quick and accurate valuations for the industry.

Further extensions and future research include but is not limited to jointly considering tax benefit incentives and the general class of Lévy processes; incorporating multiple underlying assets and pricing the lifelong version of the guaranteed minimum withdrawal benefit rider.

References

- ASIC (2012), “12-233MR ASIC reports on GFC short selling restrictions,” <http://asic.gov.au/about-asic/media-centre/find-a-media-release/2012-releases/12-233mr-asic-reports-on-gfc-short-selling-restrictions/>.
- Bacinello, A. R., Millossovich, P., and Montealegre, A. (2014), “The valuation of GMWB variable annuities under alternative fund distributions and policyholder behaviours,” *Scandinavian Actuarial Journal*, 1–20.
- Bauer, D., Kling, A., and Russ, J. (2008), “A Universal Pricing Framework for Guaranteed Minimum Benefits in Variable Annuities,” *Astin Bulletin*, 38, 621–651.
- Bernard, C. and Kwak, M. (2016), “Semi-static hedging of variable annuities,” *Insurance: Mathematics and Economics*, 67, 173–186.
- Black, F. and Scholes, M. (1973), “The Pricing of Options and Corporate Liabilities,” *Journal of Political Economy*, 81, 637–654.
- Blamont, D. and Sagoo, P. (2009), “Pricing and hedging of variable annuities,” *Cutting Edge*, 39–44.
- Carr, P., Madan, D. B., Geman, H., and Yor, M. (2002), “The Fine Structure of Asset Returns: An Empirical Investigation,” *The Journal of Business*, 2, 305–333.
- Carr, P., Madan, D. B., Melamed, M., and Schoutens, W. (2016), “Insurance : Mathematics and Economics Hedging insurance books,” *Insurance: Mathematics and Economics*, 70, 364–372.
- Chau, K. W., Yam, S. C. P., and Yang, H. (2015a), “Fourier-cosine method for Gerber-Shiu functions,” *Insurance: Mathematics and Economics*, 61, 170–180.
- (2015b), “Fourier-cosine method for ruin probabilities,” *Journal of Computational and Applied Mathematics*, 281, 94–106.
- Chen, Z. and Forsyth, P. A. (2008), “A numerical scheme for the impulse control formulation for pricing variable annuities with a guaranteed minimum withdrawal benefit (GMWB),” *Numerische Mathematik*, 109, 535–569.

- Chen, Z., Vetzal, K., and Forsyth, P. A. (2008), “The effect of modelling parameters on the value of GMWB guarantees,” *Insurance: Mathematics and Economics*, 43, 165–173.
- Coleman, T. F., Kim, Y., Li, Y., and Patron, M. (2007), “Robustly hedging variable annuities with guarantees under jump and volatility risks,” *Journal of Risk and Insurance*, 74, 347–376.
- Condron, C. M. (2008), “Variable Annuities and the New Retirement Realities,” *The Geneva Papers on Risk and Insurance-Issues and Practice*, 33, 12–32.
- Dai, M., Kuen Kwok, Y., and Zong, J. (2008), “Guaranteed minimum withdrawal benefit in variable annuities,” *Mathematical Finance*, 18, 595–611.
- Deng, G., Mccann, C., Dulaney, T., and Yan, M. (2015), “Efficient Valuation of Equity-Indexed Annuities Under Levy Processes Using Fourier-Cosine Series,” *Forthcoming Journal of Computational Finance*.
- Derman, E., Kamal, M., Kani, I., McClure, J., Pirasteh, C., and Zou, J. Z. (1998), “Investing in volatility,” *Futures and Options World*.
- Dhaene, J., Goovaerts, M. J., and Kaas, R. (2003), “Economic capital allocation derived from risk measures,” *North American Actuarial Journal*, 7, 44–56.
- Fang, F. and Oosterlee, C. W. (2008), “A Novel Pricing Method for European Options Based on Fourier-Cosine Series Expansions,” *SIAM Journal on Scientific Computing*, 31, 826–848.
- (2009), “Pricing early-exercise and discrete barrier options by fourier-cosine series expansions,” *Numerische Mathematik*, 114, 27–62.
- Feng, R. and Vecer, J. (2016), “Risk based capital for guaranteed minimum withdrawal benefit,” *Quantitative Finance*, 7688, 1–8.
- Fung, M. C., Ignatieva, K., and Sherris, M. (2014), “Systematic mortality risk: An analysis of guaranteed lifetime withdrawal benefits in variable annuities,” *Insurance: Mathematics and Economics*, 58, 103–115.
- Goudenege, L., Molent, A., and Zanette, A. (2016), “Pricing and Hedging GMWB in the Heston and in the Black-Scholes with Stochastic Interest Rate Models,” *arXiv preprint arXiv:1602.09078*, 1–38.
- Gudkov, N., Ignatieva, K., and Ziveyi, J. (2016), “Pricing of GMWB options in Variable Annuities under Stochastic Volatility , Stochastic Interest Rates and Stochastic Mortality via the Componentwise Splitting Method,” .
- Hanif, F., Finkelstein, G., Corrigan, J., and Hocking, J. (2007), “Life insurance, global variable annuities,” *Published by Morgan Stanley Research in co-operation with Milliman*.
- Heston, S. L. (1993), “A closed-form solution for options with stochastic volatility with applications to bond and currency options,” *Review of financial studies*, 6, 327–343.
- Hull, J. and White, A. (1990), “Pricing interest-rate-derivative securities,” *Review of financial studies*, 3, 573–592.
- Ignatieva, K., Song, A., and Ziveyi, J. (2016), “Pricing and Hedging of Guaranteed Minimum Benefits under Regime-Switching and Stochastic Mortality,” .
- IRI (2015), “Second-Quarter 2015 Annuity Sales Report,” <https://www.myirionline.org/docs/default-source/news-releases/iri-issues-second-quarter-2015-annuity-sales-report-%28pdf%29.pdf?sfvrsn=0>.

- Kélani, A. and Quittard-Pinon, F. (2015), “Pricing and Hedging Variable Annuities in a Lévy Market: A Risk Management Perspective,” *Journal of Risk and Insurance*.
- Kolkiewicz, A. and Liu, Y. (2012), “Semi-Static Hedging for GMWB in Variable Annuities,” *North American Actuarial Journal*, 16, 112–140.
- Kou, S. G. (2002), “A Jump-Diffusion Model for Option Pricing,” *Management Science*, 48, 1086–1101.
- Ledlie, M. C., Corry, D. P., Finkelstein, G. S., Ritchie, a. J., Su, K., and Wilson, D. C. E. (2008), “Variable Annuities,” *British Actuarial Journal*, 14, 327–389.
- Lord, R., Fang, F., Bervoets, F., and Oosterlee, C. W. (2008), “A Fast and Accurate FFT-Based Method for Pricing Early-Exercise Options under Lévy Processes,” *SIAM Journal on Scientific Computing*, 30, 1678–1705.
- Luo, X. and Shevchenko, P. V. (2014), “Fast numerical method for pricing of variable annuities with guaranteed minimum withdrawal benefit under optimal withdrawal strategy,” *International Journal of Financial Engineering*, 2, 1–24.
- Madan, D. B. and Seneta, E. (1990), “The variance gamma (VG) model for share market returns,” *Journal of business*, 511–524.
- Milevsky, M. A. and Salisbury, T. S. (2006), “Financial valuation of guaranteed minimum withdrawal benefits,” *Insurance: Mathematics and Economics*, 38, 21–38.
- Moenig, T. and Bauer, D. (2016), “Revisiting the Risk-Neutral Approach to Optimal Policyholder Behavior : A Study of Withdrawal Guarantees in Variable Annuities,” *Review of Finance*, 20, 759–794.
- Papantoleon, A. (2008), “An introduction to Lévy processes with applications in finance,” *arXiv preprint arXiv:0804.0482*.
- Peng, J., Leung, K. S., and Kwok, Y. K. (2012), “Pricing guaranteed minimum withdrawal benefits under stochastic interest rates,” *Quantitative Finance*, 12, 933–941.
- Rogers, L. C. G. and Shi, Z. (1995), “The Value of an Asian Option,” *Journal of Applied Probability*, 1077–1088.
- Ruijter, M. and Oosterlee, C. W. (2012), “Two-Dimensional Fourier Cosine Series Expansion Method for Pricing Financial Options,” *SIAM Journal on Scientific Computing*, 34, B642–B671.
- Ruijter, M., Oosterlee, C. W., and Aalbers, R. F. T. (2013), “On the Fourier cosine series expansion method for stochastic control problems,” *Numerical Linear Algebra Applications*, 20, 598–625.
- Thompson, G. W. P. (1999), “Fast narrow bounds on the value of Asian options,” Ph.D. thesis, University of Cambridge.
- Vasicek, O. (1977), “An equilibrium characterization of the term structure,” *Journal of financial economics*, 5, 177–188.
- Yang, S. S. and Dai, T.-S. (2013), “A flexible tree for evaluating guaranteed minimum withdrawal benefits under deferred life annuity contracts with various provisions,” *Insurance: Mathematics and Economics*, 52, 231–242.

A Lévy Processes

A.1 Characteristic Functions

In the following characteristic functions, μ denotes the expected return, $i = \sqrt{-1}$ is the complex unit and other parameters are specific to each process. For the risk-neutral characteristic functions we set $\mu = r + m$, where m is a drift correction term that ensures the process is a martingale under the risk measure (Fang and Oosterlee, 2008).

A.1.1 Geometric Brownian Motion (GBM)

$$\phi(\omega) = \exp\left(i\omega\mu t - \frac{1}{2}\omega^2\sigma^2 t\right),$$

$$m = 0.$$

A.1.2 Variance Gamma (VG) Process

$$\phi(\omega) = \exp(i\omega\mu t) \times \left(1 - i\omega\theta\nu + \frac{1}{2}\sigma^2\nu\omega^2\right)^{-\frac{t}{\nu}},$$

$$m = \frac{1}{\nu} \ln\left(1 - \theta\nu - \frac{\sigma^2}{2}\right).$$

A.1.3 CGMY Process

$$\phi(\omega) = \exp\left(i\omega\mu t - \frac{1}{2}\omega^2\sigma^2 t\right) \times$$

$$\exp\left(Ct\Gamma(-Y)[(M - i\omega)^Y - M^Y + (G + i\omega)^Y - G^Y]\right),$$

$$m = -C\Gamma(-Y)\left((M - 1)^Y - M^Y + (G + 1)^Y - G^Y\right),$$

where $\Gamma(\cdot)$ is the gamma function.

A.2 Cumulants

GBM	$c_1 = \mu t$ $c_2 = \sigma^2 t$ $c_4 = 0$
VG	$c_1 = (\mu + \theta)t$ $c_2 = (\sigma^2 + \nu\theta^2)t$ $c_4 = 3(\sigma^4\nu + 2\theta^4\nu^3 + 4\sigma^2\theta^2\nu^2)t$
CGMY	$c_1 = \mu T + Ct\Gamma(1 - Y)(M^{Y-1} - G^{Y-1})$ $c_2 = \sigma^2 t + CT\Gamma(2 - Y)(M^{Y-2} + G^{Y-2})$ $c_4 = Ct\Gamma(4 - Y)(M^{Y-4} + G^{Y-4}),$

(Fang and Oosterlee, 2008)

B χ and ψ functions

$$\begin{aligned}\chi_k(c, d) &= \int_c^d e^y \cos\left(k\pi \frac{y-a}{b-a}\right) dy \\ &= \frac{1}{1 + \left(\frac{k\pi}{b-a}\right)^2} \left(\cos\left(k\pi \frac{d-a}{b-a}\right) e^d - \cos\left(k\pi \frac{c-a}{b-a}\right) e^c \right. \\ &\quad \left. + \frac{k\pi}{b-a} \sin\left(k\pi \frac{d-a}{b-a}\right) e^d - \frac{k\pi}{b-a} \sin\left(k\pi \frac{c-a}{b-a}\right) e^c \right)\end{aligned}$$

$$\begin{aligned}\psi_k(c, d) &= \int_c^d \cos\left(k\pi \frac{y-a}{b-a}\right) dy \\ &= \begin{cases} \left[\sin\left(k\pi \frac{d-a}{b-a}\right) - \sin\left(k\pi \frac{c-a}{b-a}\right) \right] \frac{b-a}{k\pi}, & k \neq 0, \\ (d-c), & k = 0. \end{cases}\end{aligned}$$

(Fang and Oosterlee, 2008)

C Main Algorithms

Algorithm 1 – Static Case

Note that in the static case, the remaining guarantee account value is known at each time-step without any calculation. Also notice that there is no withdrawal at time zero. With steps referring to numerically calculating U_k coefficients numerically, note that we have used the trapezoidal rule.

1. At initialisation:
 - Calculate $G = \frac{A_0}{M}$ and $\Delta_t = \frac{t_M}{M}$.
 - Determine a and b using Equation (2.12).
 - Discretise possible investment account values $\vec{W} \in [0, W_{\max}]$ into J elements, with spacing between the elements increasing exponentially and $W_{\max} = \max[300, W_0 \cdot \exp(2b)]$.
 - Set $\vec{k} = [0, 1, \dots, N-1]$.
 - Calculate $\vec{R} = \text{Re} \left\{ \phi\left(\frac{\vec{k}\pi}{b-a}\right) \cdot \exp\left(-i\frac{\vec{k}a\pi}{b-a}\right) \right\} \cdot [\frac{1}{2} \ 1 \ \dots \ 1]'$.
2. Maturity time-step – for each element of \vec{W} :
 - Calculate y^* using Equation (2.19).
 - Calculate \vec{U} using Equation (2.18), with each element corresponding to elements of \vec{k} .
 - Calculate $V_{t_{M-1}}(W_{t_{M-1}}^-)$ as $G + \exp(-r\Delta_t) \cdot \vec{R} \cdot \vec{U}'$.
 - Store the time t_{M-1} values corresponding to each element of \vec{W} for use in the recursive step.
3. Recursive step – for t_m , where $m = M-2, \dots, 2$:
 - For each element of \vec{W} :
 - Calculate the \vec{U} coefficient vector numerically using the points where $y = \ln\left(\frac{\vec{W}}{W_{t_m^+}}\right) = \ln\left(\frac{\vec{W}}{W_{t_m^-} - G}\right)$.
 - Calculate $V_{t_m}(W_{t_m}^-)$ as $G + \exp(-r\Delta_t) \cdot \vec{R} \cdot \vec{U}'$.
 - Store the calculated values for the next recursion.
4. Time zero value:

- Calculate the \vec{U} coefficient vector numerically using the points where $y = \ln\left(\frac{\bar{W}}{W_0}\right)$.
- Calculate $V_0(W_0)$ as $\exp(-r\Delta_t) \cdot \vec{R} \cdot \vec{U}'$.

Algorithm 2 – Dynamic Case

In the dynamic case, the value must be found for different combinations of investment and guarantee account balances at each time-step. Furthermore, the optimal withdrawal strategy must be determined in the algorithm. That said, the overall structure of this algorithm is very similar to Algorithm 1.

1. At initialisation:

- Calculate $G = \frac{A_0}{M}$ and $\Delta_t = \frac{t_M}{M}$.
- Determine a and b using Equation (2.12).
- Set $W_{\max} = \max[300, W_0 \cdot \exp(2b)]$.
- Form a mesh of possible W_{t_m} and A_{t_m} values, with J elements of $W_{t_m} \in [0, W_{\max}]$, where the spacing between elements increases exponentially, and H elements of $A_{t_m} \in [0, A_0]$, which are spaced evenly.
- Set $\vec{k} = [0, 1, \dots, N-1]$.
- Calculate $\vec{R} = \text{Re} \left\{ \phi\left(\frac{\vec{k}\pi}{b-a}\right) \cdot \exp\left(-i\frac{\vec{k}a\pi}{b-a}\right) \right\} \cdot \left[\frac{1}{2} \ 1 \dots 1\right]'$.

2. Maturity time-step – for each mesh node:

- Discretise possible withdrawal amounts $\vec{\gamma}$, with spacing that matches the A direction of the mesh.
- Calculate y^* for each element of $\vec{\gamma}$ using Equation (2.19).
- Calculate matrix \mathbf{U} using Equation (2.18), which corresponds to elements of \vec{k} for each element of $\vec{\gamma}$.
- Calculate $\vec{V}_{t_{M-1}}(W_{t_{M-1}}^-, A_{t_{M-1}}^-; \gamma_{t_{M-1}}) = C(\gamma_{t_{M-1}}) + \exp(-r\Delta_t) \cdot \vec{R} \cdot \mathbf{U}$, a vector corresponding to each element of $\vec{\gamma}$.
- Set $V_{t_{M-1}}(W_{t_{M-1}}^-, A_{t_{M-1}}^-) = \sup_{\vec{\gamma}} \left[\vec{V}_{t_{M-1}}(W_{t_{M-1}}^-, A_{t_{M-1}}^-; \gamma_{t_{M-1}}) \right]$.
- Store the time t_{M-1} values for use in the first recursive step.

3. Recursive step – for t_m , where $m = M-2, \dots, 2$:

- For each mesh node
 - Discretise possible withdrawal amounts $\vec{\gamma}$, with spacing that matches the A direction of the mesh.
 - Calculate matrix \mathbf{U} numerically using Equation (2.17), which contains a vector corresponding to elements of \vec{k} for each element of $\vec{\gamma}$.
 - Calculate $\vec{V}_{t_m}(W_{t_m}^-, A_{t_m}^-)$ as $C(\gamma_{t_m}) + \exp(-r\Delta_t) \cdot \vec{R} \cdot \mathbf{U}$.
 - Set

$$V_{t_m}(W_{t_m}^-, A_{t_m}^-) = \sup_{\vec{\gamma}} \left[\vec{V}_{t_m}(W_{t_m}^-, A_{t_m}^-; \gamma_{t_m}) \right]. \quad (\text{C.0})$$

- Store the calculated values for the next recursion.

4. Time zero value:

- Calculate the \vec{U} coefficient vector numerically using points where $y = \ln\left(\frac{\bar{W}}{W_0}\right)$.
- Calculate $V_0(W_0, A_0) = \exp(-r\Delta_t) \cdot \vec{R} \cdot \vec{U}'$.